SYNTHESIS AND DEVELOPMENT OF SMALL MOLECULE INHIBITORS TARGETING VIRAL PA_N ENDONUCLEASE AND BACTERIAL MreB

By

RAJLAKSHMI SAWANT

A thesis submitted to the

School of Graduate Studies

Rutgers, The State University of New Jersey

In partial fulfillment of the requirements

For the degree of

Master of Science

Graduate Program in Medicinal Chemistry

Written under the direction of

Dr. Edmond J. LaVoie

And approved by

_____

_____

_____

_____

New Brunswick, New Jersey

May, 2018

ABSTRACT OF THE THESIS

SYNTHESIS AND DEVELOPMENT OF SMALL MOLECULE INHIBITORS TARGETING VIRAL PA_N ENDONUCLEASE AND BACTERIAL MreB

By RAJLAKSHMI SAWANT

Thesis Director:

Edmond J. LaVoie, Ph.D.

Imminent threat of pandemics of influenza, along with increasing resistance of the virus to existing anti-viral drugs has posed a need for development of an anti-viral that possesses a novel mechanism of action. PA_N Endonuclease enzyme protein plays an important role in influenza A viral transcription with the cap-snatching process being highly conserved in the virus. This makes PA_N an attractive target for drug development.

Our efforts began with fragment screening to identify an effective pharmacophore. 5-chloro-3-hydroxypyridin-2(1*H*)-one was identified as a highly active chelating ligand at the endonuclease site containing metal ions. After extensive research, 3-hydroxypyridin-2(1*H*)-ones, 3-hydroxyquinolin-2(1*H*)-ones and aza analogs of 3-hydroxypyridin-2(1*H*)-ones

were prepared which displayed modest enzymatic inhibitory activity. This activity didn't translate in the cellular assay. Hence, we synthesized a known endonuclease inhibitor (Shionogi Co.) to check whether the established structure activity relationships were "false-positive" data. We also experimented with the development of isatin derivatives to continue the search for a lead compound. The most promising compound, 6-Bromo-1-hydroxyindoline-2,3-dione showed 45% inhibition at 200 μM concentration. This molecule was optimized to give 6-(4-fluorophenyl)-1,3-dihydroxy-3-methylindolin-2-one which showed no inhibitory activity in the enzyme assay. Despite of unsuccessful attempts, continued efforts are being made to explore PA_N as a potential target for antiviral therapy.

Our research efforts were then directed towards tackling another emerging global health crisis, the antibiotic resistance crisis. With increasing bacterial strains developing resistance towards currently available antibiotics, there is a need to target a novel mechanism of action in bacteria. MreB, a highly conserved actin homologue in bacteria is important in cell wall synthesis and determining the cell shape in bacteria. The significance of MreB in bacterial cell growth makes it a lucrative target for design of antibiotics.

A22 was identified as an MreB inhibitor with modest inhibitory activity. Our efforts were focused on studying the structure activity relationships by modifying the aromatic core of A22. A series of benzothiophene, benzofuran and indole based isothioureas was synthesized. Deductions made from SAR studies are currently being used to develop an optimized lead that can show substantial MreB inhibitory activity and can further be developed into clinic.

ACKNOWLEDGEMENT

Firstly, I would like to express deep gratitude to my advisor, Dr. Edmond J. LaVoie. Your constant mentorship, guidance, patience and belief in my skill are the reasons why I have managed to finish this thesis. You are an everlasting inspiration for me as a researcher and I cannot thank you enough for making these three years of learning an enriching experience.

Secondly, I would also like to express my gratitude to my thesis committee members, Dr. Longqin Hu and Dr. Joseph E. Rice. I would like to thank all members of TAXIS Pharmaceuticals, Dr. Joseph D. Bauman and Jia Han for extensively helping me with the biological testing of compounds in this project.

I would further extend my thanks to Dr. Gifty Blankson and Dr. Hye Yeon Sagong, my lab mates. I could not have asked for better mentors to train me in lab and provide me solid support during challenging times in the lab. I specially would like to thank Elissa Glinn for her kind presence in helping me out with even the smallest of issues during my three years of education at Rutgers. Also, my gratitude extends to all the members of the department of Medicinal Chemistry and all my friends for their unwavering friendship.

Finally, the biggest thank you to my parents, Hemant Sawant and Purva Sawant. You give me constant motivation to become a better human everyday and you are my everything. Thank you.

DEDICATION

Dedicated to my mom and dad.

TABLE OF CONTENTS

LIST OF TABLES

LIST OF FIGURES

LIST OF SCHEMES

CHAPTER 1

PA_N Endonuclease Inhibitors

Introduction

Influenza virus is the most common causative agent of respiratory tract infections in humans. Influenza outbreaks, in the form of both epidemics and pandemics, have been occurring for centuries causing high disease and fatality rates in densely populated areas. The 1918 pandemic Spanish Flu was one of the deadliest outbreaks of Influenza (H1N1 subtype) causing 50-100 million deaths worldwide.[1] Currently, every endemic season in the USA sees about 36,000 deaths and around 200,000 morbidities due to influenza infection.[2,3]

Historically, there have been two major classes of anti-influenza agents. These consisted of M2 ion channel blockers and neuraminidase (NA) inhibitors. The two M2 channel blockers in clinical use in the United States are adamantine and rimantadine. It is believed that M2 ion channel blockers primarily prevent the release of infectious viral nucleic acid into the host cell by interfering with the transmembrane domain of the viral M2 protein.[4] Amantadine is also known to prevent viral assembly during replication.[4] Amantadine inhibits the replication of influenza A virus isolates from each of the subtypes (ie, H1N1, H2N2 and H3N2), but has very little or no activity against influenza B virus isolates. Rimantadine exerts its inhibitory effect on three antigenic subtypes of influenza A virus (H1N1, H2N2, H3N2) early in the viral replicative cycle, possibly inhibiting the uncoating process and exposing its contents to the cytoplasm of the host cell.[4,5] While rimantadine is two- to eightfold more active than amantadine, it too has no activity against

influenza B virus. Resistant mutant strains are known to develop quickly to these M2 ion channel blockers and several influenza A virus strains have been increasingly observed in the clinic.[5] Neuraminidase (NA) inhibitors have proved useful as agents that could be used to limit the spread of influenza infection. Neuraminidase is a glycoside hydrolase enzyme that participates in the release of the virus from the host cell.[6] Inhibition of neuraminidase inhibitors prevents the efficient releases of virus progeny from infected host cells, which results in a limitation of the severity and spread of viral infections.[4,7] There are three NA inhibitors in clinical use in the United States. These are oseltamivir (Tamiflu®), zanamivir (Relenza®) and peramivir (Rapivab®). For several years, these agents have been viewed as first-line treatment for the prevention of the spread of influenza infections. However, strains of influenza A virus resistant to oseltamivir and other NA inhibitors are beginning to surface.[7] In addition, for maximal efficacy, these agents need to be administered within 48 hours of infection.[7] Considering all these factors, there remains a dire need for the development of novel antiviral agents which can counter resistance and can be used in the prevention and treatment of influenza virus infections and pandemics.

A third major class of new antiviral agents has very recently been identified and validated. Specifically, these agents target an essential endonuclease of the influenza virus.[8] Metal chelators like L-735,882 and flutimide (Figure 1) have been recognized as potential endonuclease inhibitors acting by metal chelation at the active site. The first member of this class, baloxavir marboxil, has been approved on February 23, 2018 for clinical use in Japan. This agent, which was initially developed by Shionogi Inc. and licensed by Roche Pharma, successfully targets the same enzymatic process as the new structural chemical entities described in this Thesis. These timely results validate the target

that was central to our studies towards the development of novel antiviral agents for treating influenza A and B infection.

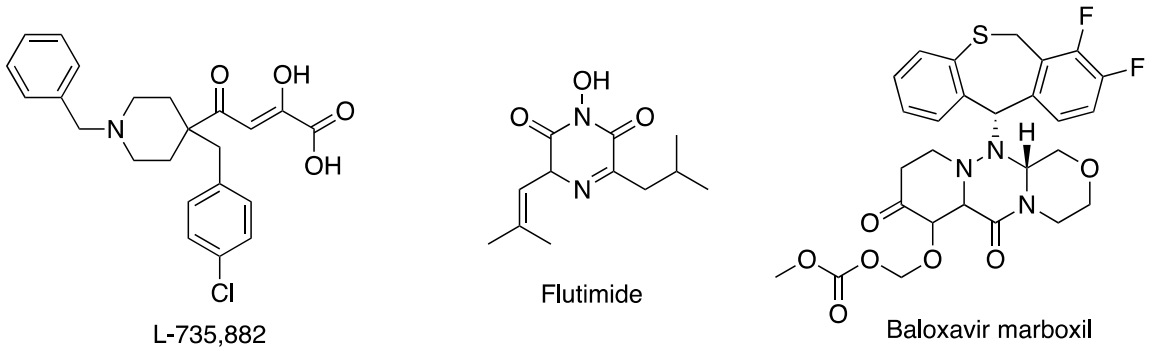

Figure 1. Known endonuclease inhibitors

Influenza viruses can be categorized into 4 subtypes: A, B, C, D. Types A and B are responsible for the seasonal epidemics seen in humans.[1] Type A viruses are further sub-categorized based on proteins present on the viral surface, hemagglutinin (18 subtypes) and neuraminidase (11 subtypes). Influenza virus is a single stranded virus with a negative sense genome belonging to family Orthomyxoviridae.[9] The genome is comprised of 8 distinctive viral RNA (vRNA's) segments, together encoding a total of 11 viral proteins.[9] These segments exchange among viruses inside infected host cells. Once the vRNA enters the infected host nucleus, RNA-dependent RNA polymerase (RdRp) enzyme acts as a catalyst for transcription and replication.[3,9]

Structure of PA_N Subunit of RdRp

The heterotrimer of RdRp exists as 3 subunits: PA (acidic), PB1 and PB2 (basic) within the virus.[9] These subunits, together with the nucleoproteins and vRNA constitute the viral ribonucleoprotein (vRNP) and glycoproteins, hemagglutinin (HA) and neuraminidase (NA).[9] The PA subunit is 80-kDa and upon trypsin digestion, it undergoes cleavage into two domains: a larger ~55 kDa C-terminal domain (198-716 residues) and a smaller ~25 kDa N-terminal domain. The N-terminal domain (1-197 residues) called PA_N is responsible for endonuclease enzymatic activity.[9]

Elucidation of crystal structure of PA_N, as shown in ribbon form in Figure 2, revealed that its core structure resembles proteins belonging to the diverse PD-(D/E)XK phosphodiesterase superfamily.[9,10] A folded PA_N domain consists of seven α-helices which surround β-strands (five in number). These seven α-helices, in turn, form a twisted planar scaffold. A highly negatively charged depression houses a metal cation that coordinates with active site amino acid residues. The active site is the cation-dependent endonuclease enzyme. Although confusion still persists on the type and quantity of metal cations present, it is believed that 1-3 manganese or magnesium ions coordinate with residues in the active site. Residues that engaged in conserved cation binding were identified as histidine His41, acidic amino acids Glu80, Glu119 and Asp108 with catalytic lysine residue Lys134.[9,10]

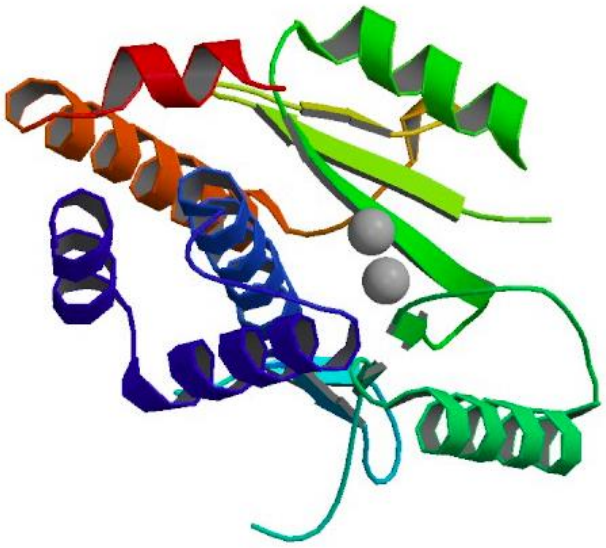

Figure 2. Ribbon structure of PA_N (PDB: 4AVQ)[24]

The two-metal-cation model is widely supported by substantial biochemical data.[10] However, there has been recent data that indicates existence of a third metal in the endonuclease active site of PA_N.[10] It is suggested that, metal I assists in catalysis, metal II provides support to the structure and metal III acts as a charge stabilizer during the cleavage of host mRNA.

Viral Transcription involving RdRp

Studying transcription and replication of the viral genome as well as the role of RNA-dependent RNA polymerase (RdRp) in the process are crucial to understanding why RdRp is an attractive target for development of inhibitors of influenza replication. Viral RdRp initiates and facilitates transcription.[10,11] RdRp binds to 5' and 3' terminal sequences of the vRNA genome segments to form viral ribonucleoprotein (vRNP) complexes. RdRp assumes a cis acting model to catalyze transcription as opposed to the trans model for replication. These 5' and 3' ends of the vRNA segments are conserved and exhibit inverted

complementarity in the sequences. Further, the vRNA promoter upon associating with RdRp, gets oriented in a double helical loop, which plays a vital role in regulating transcription.

Synthesis of mRNA occurs inside the infected cell's nucleus by direct copying from the vRNA template. This process, however, is primer dependent. 5'-capped mRNA segment acts as the primer here. RdRp is incapable of synthesizing its own 5'-cap which is why it enables hijacking of 5'-capped mRNA segments from the host pre-mRNAs.[11,12] This process is called 'cap-snatching' and it is a critical step in the lifecycle of influenza virus. Cap-snatching begins when the PB2 subunit of RdRp binds to the host pre mRNA cap. This cap contains a phosphodiester bond 10-13 nucleotides downstream, which is cleaved by endonuclease residing in the N-terminal of PA subunit.[11,12] Transcription proceeds by using the viral genome as a template, with elongation occurring in 3' to 5' direction and through the active site of PB1 subunit. This continues until RdRp reaches an oligo(U) sequences containing 5-7 U residues, situated about 16 nucleotides away from the 5' terminus of vRNA template. This sequence is a cue for polyadenylation of mRNA. Finally, the synthesized mRNA is released from PB2 subunit by template slipping resulting in capped and polyadenylated positive sense mRNA which are transported to the cytoplasm for translation by the eukaryotic host cell. The complete mechanism has been illustrated in Figure 3.[13]

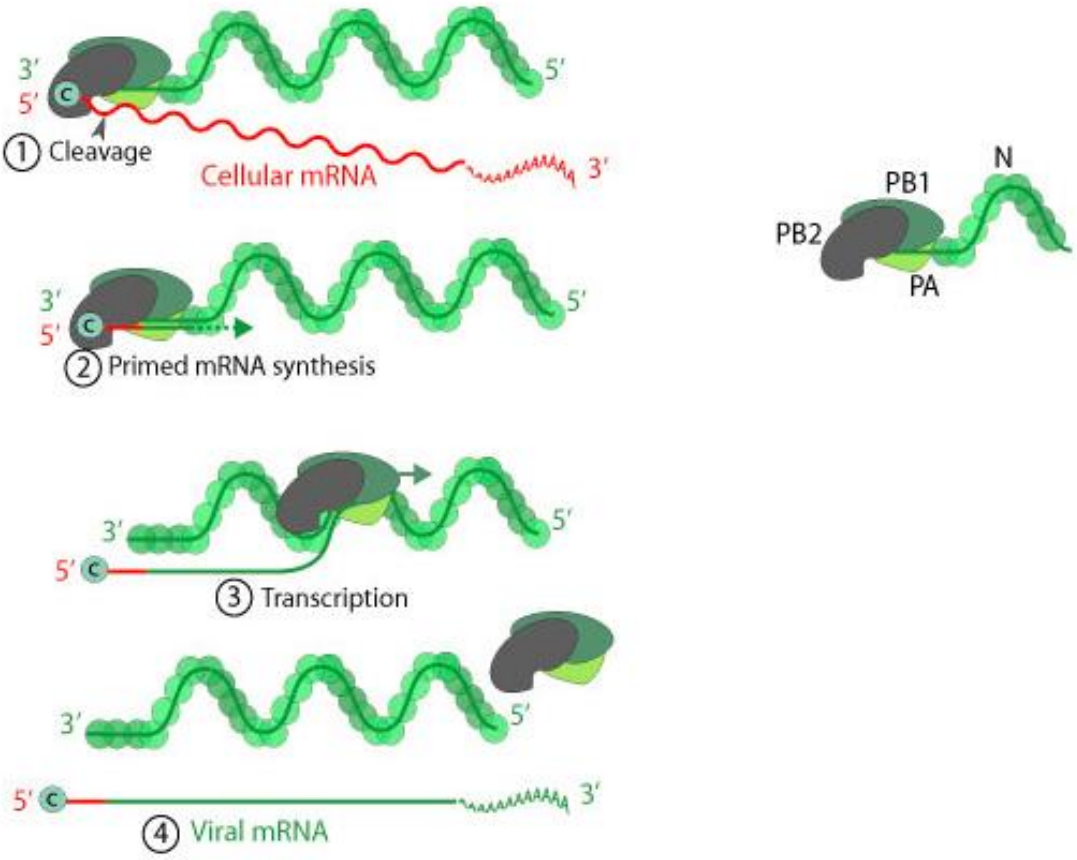

Figure 3. Cap-snatching mechanism[13]

The structure and function of RdRp and its importance in influenza A virus transcription and replication have supported the assertion that it is an attractive target for development of new antiviral agents. This had been a largely unexploited area of research. The development of agents that could inhibit this enzymatic process would bypass existing resistance mechanisms and emergence of new mutant strains is unlikely. In addition, since cap snatching is a process exclusive to the virus and absent in human cells, these antiviral agents will not be expected to interfere with the human cell life cycle. More specifically, inhibitors that target endonuclease activity have garnered even more attention owing to the novelty of the mechanism. Deduction of structure of PA_N showed presence of divalent

metal cations (Mg^{2+} and Mn^{2+}) in a deep cavity in the endonuclease active site. Compounds that can chelate to these metal ions and thereby inhibit endonuclease present an innovative approach in the designing of antiviral agents.

Background for Shionogi Compound[17]

Endonuclease activity as a potential target for inhibition had been an untapped territory until the approval of baloxavir marboxil (Xofluza®), whose structure is illustrated in Figure 1. After extensive studies were done on RNA polymerase endonuclease and its importance in viral cell replication and life-cycle, enough data was obtained to support the idea that PA_N can be effectively targeted to design new agents against influenza. Inhibitors designed to target endonuclease should show robust *in vitro* as well as *in vivo* anti-viral activity. Considering these factors, we began our efforts with screening fragments from a library containing a diverse pool of compounds using X-ray crystallography techniques. A total of 775 Fragments were screened initially by soaking fragments into preformed protein crystals. Of these 159 compounds were found to have metal chelating groups and 8 of those effectively inhibited PA_N. 5-Chloro-3-hydroxypyridin-2(1*H*)-one (**1**) and 5-bromo-2-hydroxypyridin-2(1*H*)-one (**2**) were two of the 8 initial hits with IC_{50} values of 25 μM and 16 μM respectively, as shown in Table 1.[14,15]

	Compound Structure	IC_{50} (μM)
1	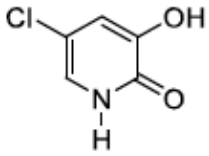	25
2	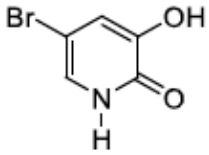	16

Table 1. Biological activities of **1** and **2**

Further structural modifications lead to development of three series of compounds; 3-hydroxypyridin-2(1*H*)-ones, 3-hydroxyquinolin-2(1*H*)-ones and aza analogs of 3-hydroxypyridin-2(1*H*)-ones. The most promising analog with modest *in vitro* and *ex vivo* activity was found to be compound **3**, whose structure has been shown in Figure 4. However, none of the other compounds in any of these three series of compounds showed any *ex vivo* activity despite exhibiting *in vitro* activities comparable to compound **3**.[14,15, 16]

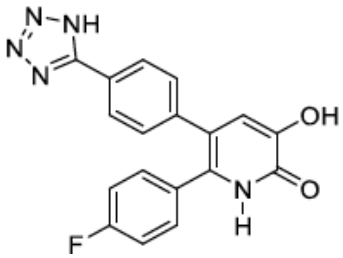

Figure 4. Structure of Compound **3**

Based on these results, it was hypothesized that the misleading discrepancy in the *in vitro* vs *ex vivo* activities is due to usage of an *in vitro* assay that used a truncated endonuclease enzyme and not the entire viral RNP complex. This may give rise to false positive derivatives that would mislead the structure-activity relationships that were

developed and result in derivatives with potent *in vitro* activity, but not exhibit efficacy in an *ex-vivo* bioassay. In order to validate this conjecture, we began the synthesis of compound **4** (shown in Figure 5), which is a robust endonuclease inhibitor from Shionogi Co.,[17] with a reported IC_{50} of 1.4 nM and EC_{50} of 37 nM.

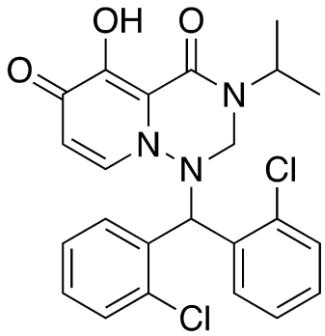

Figure 5. Structure of Compound **4**

Results and Discussion

The initial methodology employed for the synthesis of compound **4** was gleamed from the Shionogi patent.[17] Synthesis of compound **4** involved a series of 8 reactions starting from commercially available maltol, **4a**. Treatment of **4a** with benzyl bromide (1 eq.), under basic conditions, provided **4b** in quantitative yield (Scheme 1). The 3-hydroxyl group was protected so as not to interfere in subsequent reactions.

Scheme 1. Synthesis of **4b**

The methyl group at 2 position was oxidized using selenium dioxide (6 eq.) to give aldehyde **4c** in 63% yield (Scheme 2).

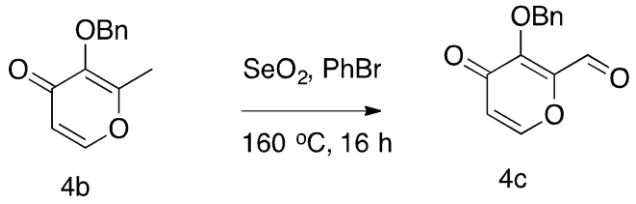

Scheme 2. Synthesis of **4c**

The aldehyde formed in the previous step was further oxidized using sodium chlorite and sulfamic acid as the by-product scavenger to an acid **4d** in 72% yield (Scheme 3).

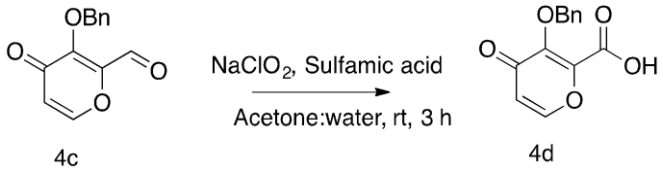

Scheme 3. Synthesis of **4d**

The pyrone ring in **4d** was converted to a pyridone **4e** in 80% yield using excess aqueous ammonia (Scheme 4).

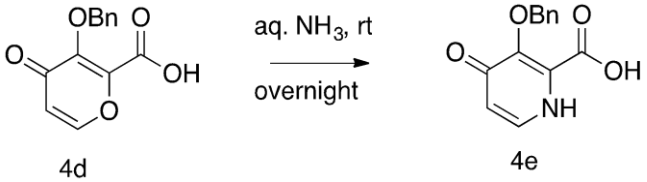

Scheme 4. Synthesis of **4e**

Then **4e** was coupled with isopropylamine using WSC.HCl and hydroxybenzotriazole to yield 55% of amide **4f** (Scheme 5).

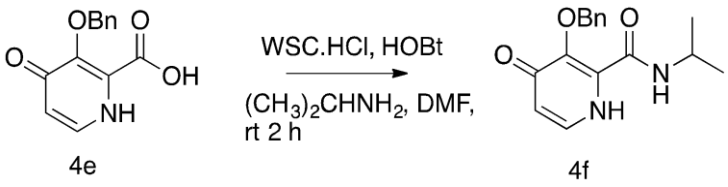

Scheme 5. Synthesis of **4f**

The ring nitrogen of **4f** was treated further with O-(2,4-dinitrophenyl)hydroxylamine under basic conditions to yield 52% of 1-hydrazone **4g** (Scheme 6).

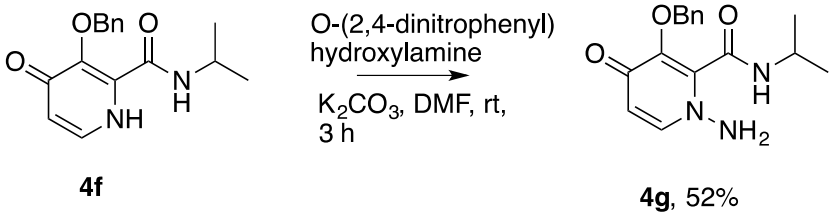

Scheme 6. Synthesis of **4g**

The hydrazine **4g** was cyclized using paraformaldehyde and acetic acid as a catalyst to yield 76% of triazine bicycle **4h** (Scheme 7).

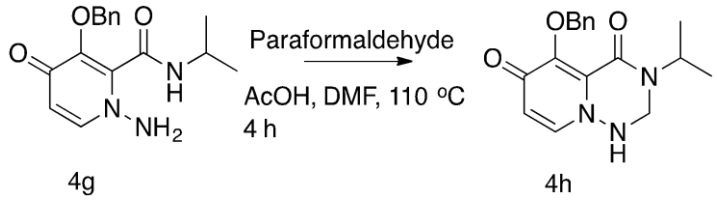

Scheme 7. Synthesis of **4h**

The reaction conditions for the final step, which involves nucleophilic substitution, included treatment with 96% sulfuric acid, as illustrated in Scheme 10. This was viewed as relatively harsh reaction conditions. When the product of this reaction was analyzed

using Nuclear Magnetic Resonance (NMR), the proton spectrum showed a messy aromatic region despite of absence of other impurities. It was thus concluded from these initial reactions attempts that we should explore milder reaction conditions. Hence, we decided to explore alternative procedures to enable substitution and then subsequent deprotection. The reaction conditions along with observed results have been tabulated in Table 2.

METHODS USED	CONDITIONS TRIED	RESULTS
1. Use of base and alkyl halide (Substitution)	Bases used - Sodium Hydride, Cesium Carbonate (1-3 eq.) Temperature: RT to 100 degrees Duration - 2 hours to overnight Starting material – **4g/4h**	No reaction observed with use of a mild base like cesium carbonate with either starting material. Reaction with sodium hydride resulted in fragmentation of starting material within an hour Temperatures above 100 °C resulted in ring opening, amide **4f** recovered in one experiment.
2. Reductive animation using bis(2-chlorophenyl)methanone	Base – Sodium acetoxyborohydride Starting material – **4g/4h**	No reaction observed, starting material recovered
3. Simultaneous alkylation and deprotection using strong acid and bis(2-chlorophenyl)methanol	Literature procedure – Acetic acid and conc. Sulfuric acid, with ethanol as solvent	reported yield 29% observed yield 13%

Table 2. Overview of conditions tried for synthesis of **4**

Reacting **4g** and **4h** separately using 2,2'-(bromomethylene)bis(chlorobenzene) and cesium carbonate (1-3 eq.) resulted in no reaction. Increasing the temperature, when reacting **4h** with the halide and cesium carbonate, to 100 °C resulting in ring-opening and provided the amide **4f**, suggesting loss of methylamine. We then used a stronger base sodium hydride with the logic that maybe cesium carbonate was a not strong enough base

to deprotonate the free amine of **4g** or cyclic amine, **4h**. Use of NaH resulted in decomposition of starting material **4g** as well as **4h** within one hour (Scheme 8).

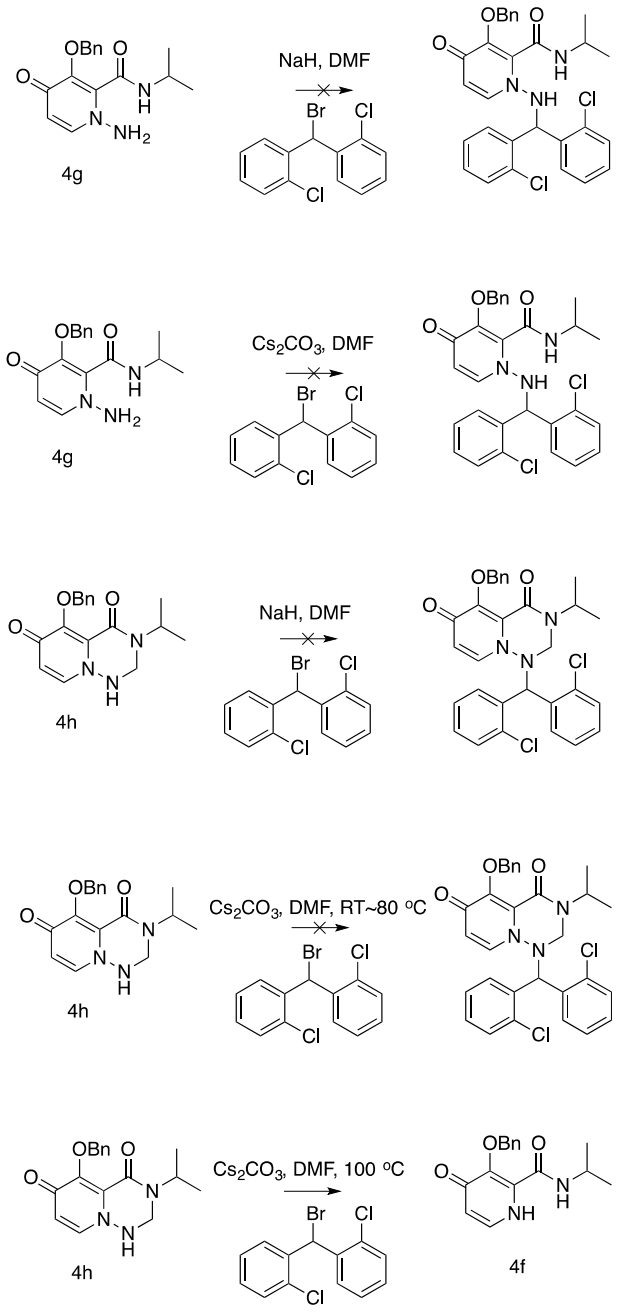

Scheme 8. Alternative schemes tried for synthesis of **4**

The next approach we tried was a one-pot reductive amination, using sodium triacetoxyborohydride as the reducing agent, on two substrates **4g** and **4h**. However, both the substrates remained unreacted (Scheme 9).

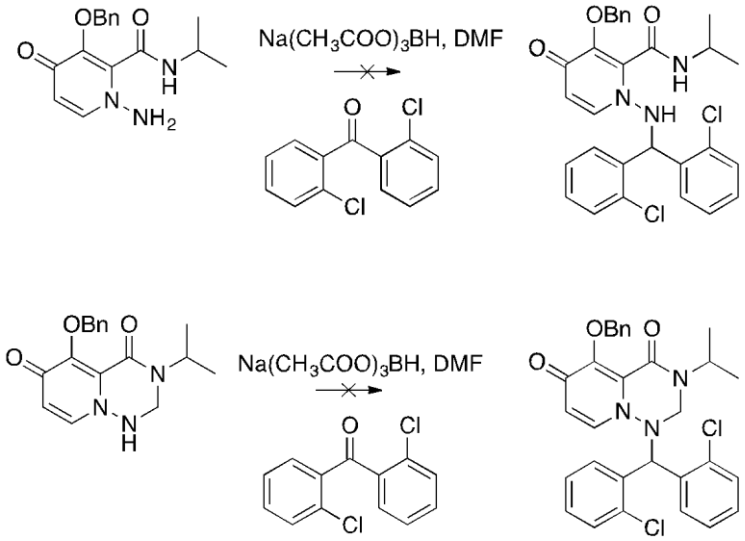

Scheme 9. Reductive amination – alternative route for synthesis of **4**

Finally, we revisited the original approach and resorted to using 96% sulfuric acid in acetic acid (Scheme 10). The temperature was strictly controlled and the reaction was run for 2 hours. In addition, instead of filtering the product precipitate as given in the literature procedure, we extracted the reaction mixture with ethyl acetate and washed the organic layer with water to remove impurities. Purification of the dried organic layer afforded the desired compound **4** in 13% yield as a bright orange free-flowing powder.

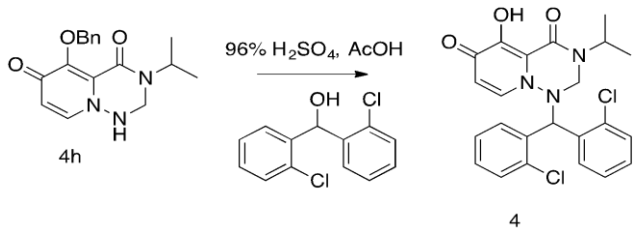

Scheme 10. Final synthesis of **4**

Compound **4** was found upon testing in a Fluorescence Resonance Energy Transfer (FRET) based *in vitro* assay and Fluorescence Forming Units (FFU) based *ex vivo* assay to be a potent endonuclease inhibitor with activity comparable to that reported in literature, thereby giving a confirmatory answer to our experimental hypothesis. The high-throughput *in vitro* assay was carried out based on a 96-well plate FRET based assay. The fluorophore used was 6-carboxy-fluorescein (FAM) which, upon cleavage from 5'-end of TaqMan-like oligonucleotide, fluoresced when excited using a 488 nm wavelength light. A nonfluorescent quencher (MGBFNQ, Applied Biosystems) was present at the 3'-end of the oligonucleotide. Change in fluorescence was measured for compound **4** and IC_{50} was calculated.[16] This has been depicted in Figure 6.[16]

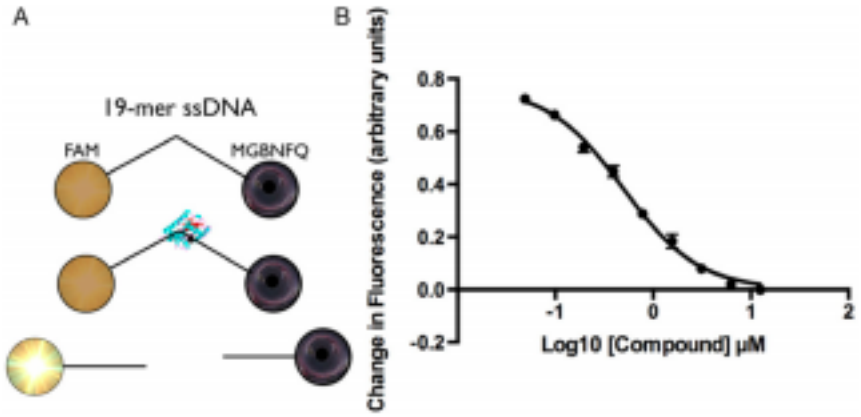

Figure 6. Details of FRET based enzymatic assay

The *ex vivo* activity was evaluated by a virus yield assay in Madin-Darby Canine Kidney (MDCK) cells. FFU assays were used to determine virus titers in supernatents after an infection of 24 hours at various compound concentrations. Oseltamivir and DMSO were used as positive and negative control, respectively. These data indicate that our *in vitro* could detect agents that would ultimately have *ex-vivo* antiviral activity.

Unfortunately, it was also giving rise to "false-positive" responses, wherein a significant number of compounds, such as 3-hydroxy-2-pyridinone derivatives with exceptional activity in our *in vitro* assay, failed to exhibit any significant *ex-vivo* activity.

Synthesis and development of isatin analogs

Studies were done on 3-hydroxypyridin-2(1*H*)-ones by Dr. Ajit Parhi and further optimization studies were done to develop 3-hydroxyquinolin-2(1*H*)-ones and aza analogs of 3-hydroxypyridin-2(1*H*)-ones by Dr. Hye Yeon Sagong which showed acceptable inhibition against endonuclease *in vitro*.[14,15,16] This led to a building of SAR which illustrates functional groups that are required for optimum binding in the endonuclease

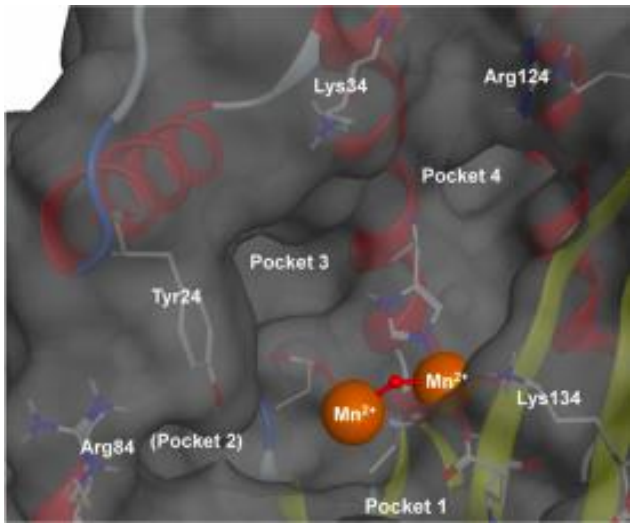

Figure 7. AA residues at endonuclease binding site.[10]

binding site, chelation with the Mg^{2+} and Mn^{2+} ions and consequently inhibition of endonuclease. The amino acid (AA) residues present at the binding site have been illustrated in Figure 7.[10]

The following were the key interactions that could be derived from the SAR studies:

1. A heterocyclic hydrophobic scaffold like pyridine or quinolone with the presence of 2-3 chelator functionalities was necessary
2. Another hydrophobic moiety extending from 5^{th} or 6^{th} position of the heterocyclic ring, especially 4-fluorophenyl ring lead to increased inhibitory activity, possibly due to cationic pi interactions with M3
3. A hydroxyl group at the 3^{rd} position of the heterocycle showed good chelation and hence better IC_{50} over non-hydroxy counterparts

However, due to a lack of *ex vivo* activity associated with these compounds despite major increase *in vitro* potency, we decided to explore a new scaffold that potentially could meet all the requisites of a novel anti-viral drug candidate.

Isatins presented a novel and interesting target for subsequent exploration. Our studies began with commercially available indoline-2,3-dione (isatin) derivatives. The target compounds are outlined in Scheme 11.

Reduction of carbonyl group on the third position using 1.0 equivalent sodium borohydride gave a 3-hydroxyindolin-2-one **5** which was tested for inhibitory activity in endonuclease enzyme using FRET based *in vitro* assay. The idea behind this set of compounds was that the 2-carbonyl and 3-OH groups engaged in chelation with the Mg^{2+} and Mn^{2+} ions in endonuclease active site. It was found to have no inhibitory activity on endonuclease. Further, based on the SAR developed earlier on 3-hydroxypyridin-2(1*H*)-ones, reduction of commercially available bromo substituted isatins was pursued to obtain compounds **6-9**.

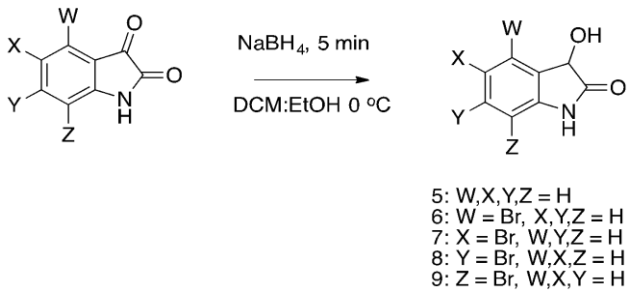

Scheme 11. Synthesis of **5-9**

	Compound Structure	IC_{50} (μM)
5	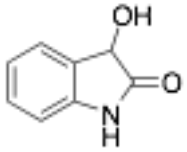	>100
6	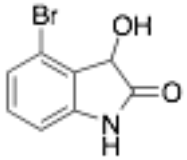	>100
7	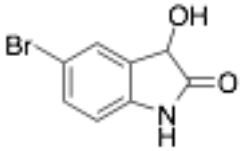	>100
8	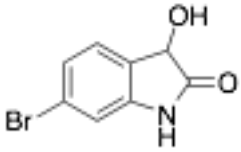	>100
9	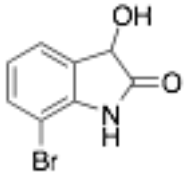	>100

Table 3. Biological activity of **5-9**

These compounds also failed to show endonuclease inhibitory activity in the *in vitro* assay as shown in Table 3.

SAR studies indicated that substitution by aryl groups on 5 or 6 position of 3-hydroxy-2-pyridinones increased activity. In view of these data, we decided to study the effect of 4-fluorophenyl substitution on 4, 5, 6 and 7 positions, respectively, of the isatin ring. These compounds were synthesized as outlined (Scheme 12).

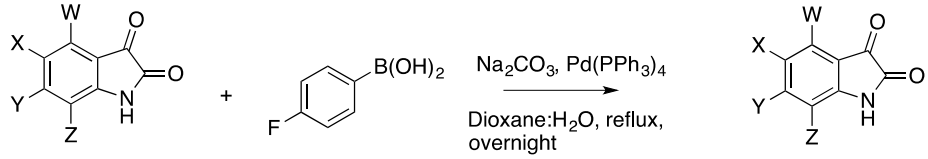

10a: W = Br, X,Y,Z = H (10%)
11a: X = Br, W,Y,Z = H (43%)
12a: Y = Br, W,X,Z = H (12%)
13a: Z = Br, W,X,Y, = H (45%)

10: W = 4-fluorophenyl, X,Y,Z = H (10%)
11: X = 4-fluorophenyl, W,Y,Z = H (43%)
12: Y = 4-fluorophenyl, W,X,Z = H (12%)
13: Z = 4-fluorophenyl, W,X,Y, = H (45%)

Scheme 12. Synthesis of **10-13**

All four of the positional isomers of 4-fluorophenylisatin, as depicted in Scheme 12 were prepared and evaluated in the *in vitro* assay. IC_{50} values of **10-14** have been tabulated in Table 4.

	Compound Structure	IC_{50} (μM)
10	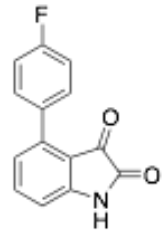	>100
11	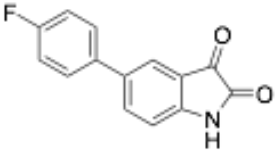	>100
12	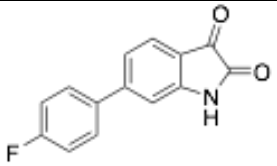	>100
13	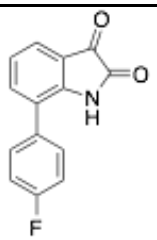	>100

Table 4. Biological activity of **10**-**13**

However, these modifications failed to result in any significant inhibition in the enzymatic assay. Based on the binding requirements and enzymatic interactions in the endonuclease active site, it was further decided that it was important to extend these studies to molecules 3-hydroxy-2-indol-2-ones, which more closely resembled the 3-hydroxy-2-pyridinone series previously investigated.

A Grignard reaction was carried out using methyl magnesium bromide (1.0 eq) to give a tertiary alcohol at the 3rd position to give compounds **14** and **15** (Scheme 13).

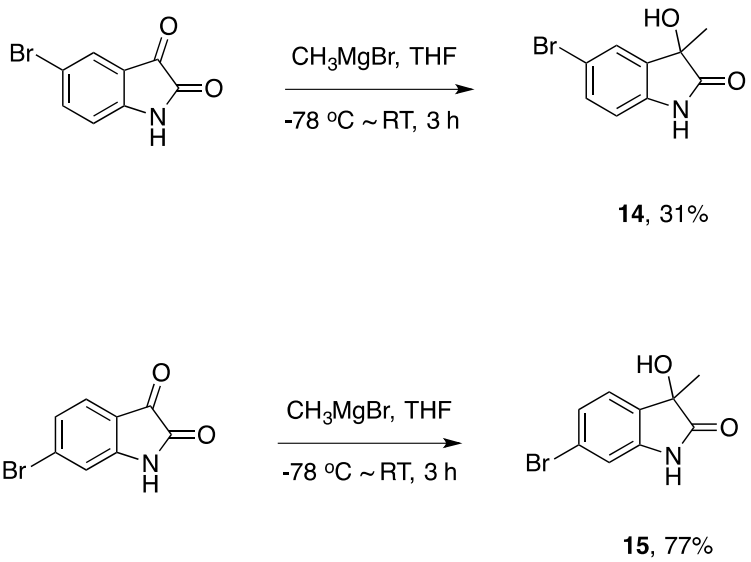

Scheme 13. Synthesis of **14** and **15**

Subjecting **14** to Suzuki coupling using 4-fluorophenyl boronic acid did not give the desired coupled product (Scheme 14). Protection of the indole nitrogen was thought to be required prior to attempting the Suzuki coupling.

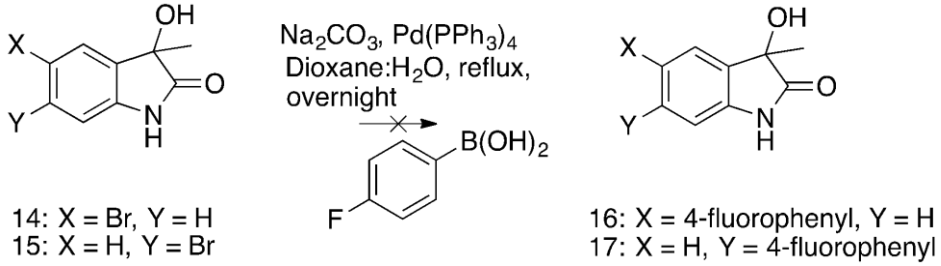

Scheme 14. Attempted synthesis I of **16** and **17**

We experimented with a range of protecting groups. Benzyl protection went ahead successfully in quantitative yield on 6-bromoisatin. Grignard reaction on **Ib** and Suzuki coupling on **Ic** was also successful. However, removal of the N-benzyl group proved to be

difficult. Deprotection using hydrogenation on Pd/C or $Pd(OH)_2$ proved ineffective (Scheme 15).

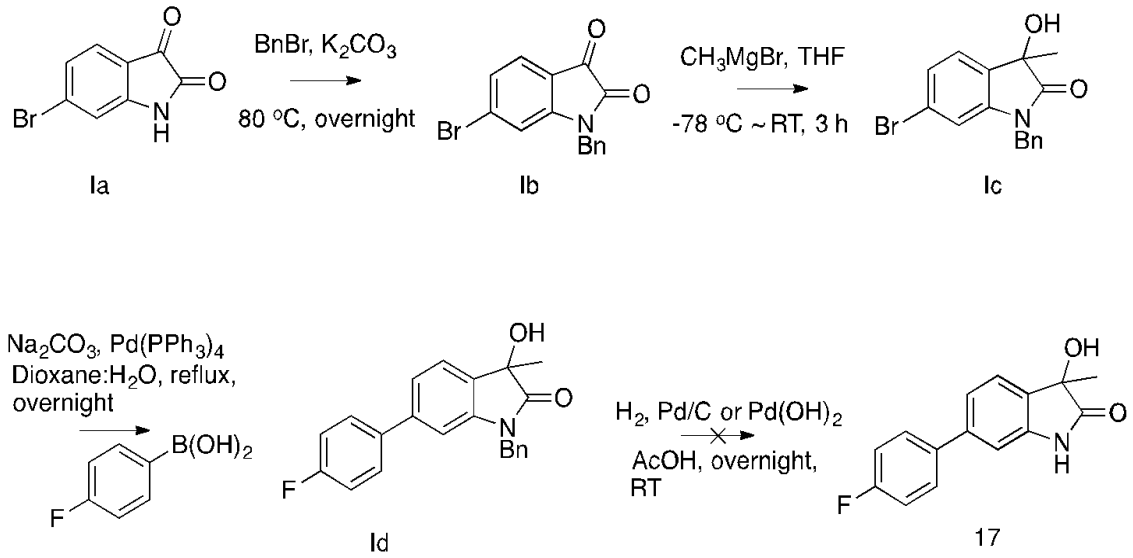

Scheme 15. Attempted synthesis II of **17**

We switched to the more sensitive *p*-methoxy benzyl (PMB) group and went ahead with the same scheme of synthesis.[20] Deprotection of PMB was also unsuccessful using hydrogenolysis conditions (Scheme 16).

Hence, we decided to switch to silyl groups which are more labile to deprotection. To maximize the yield, we wanted to minimize the number of steps in the scheme and for this reason in-situ protection using the sensitive TMS group was considered to be the best

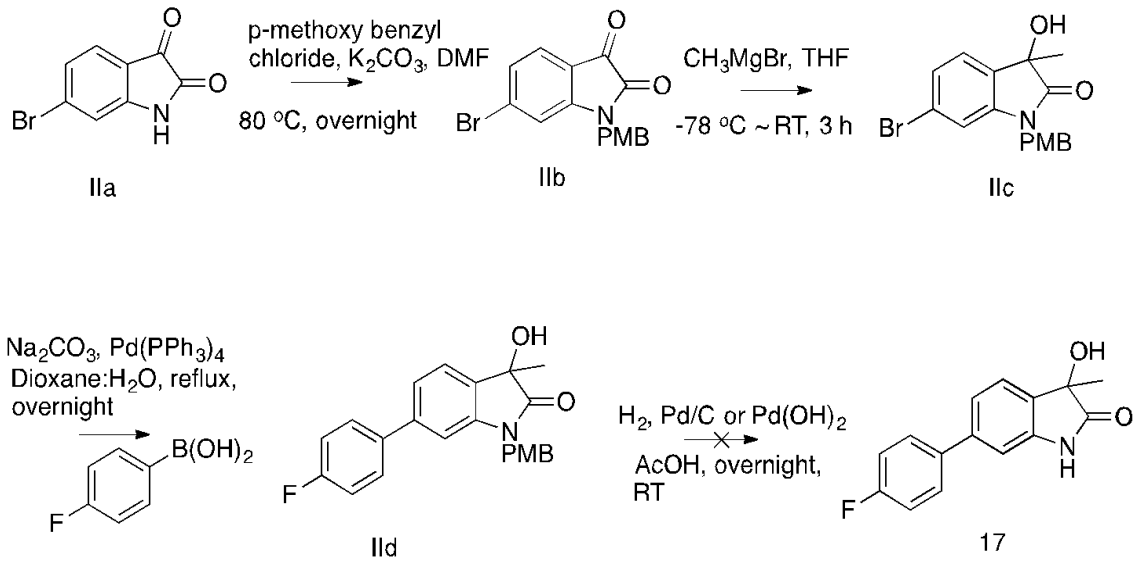

Scheme 16. Attempted synthesis III of **17**

option to pursue. Temporary TMS protection using TMSCl was done and crude from this step was directly used for Suzuki coupling using 4-fluorophenyl boronic acid to give compounds **16** and **17** (Scheme 17).

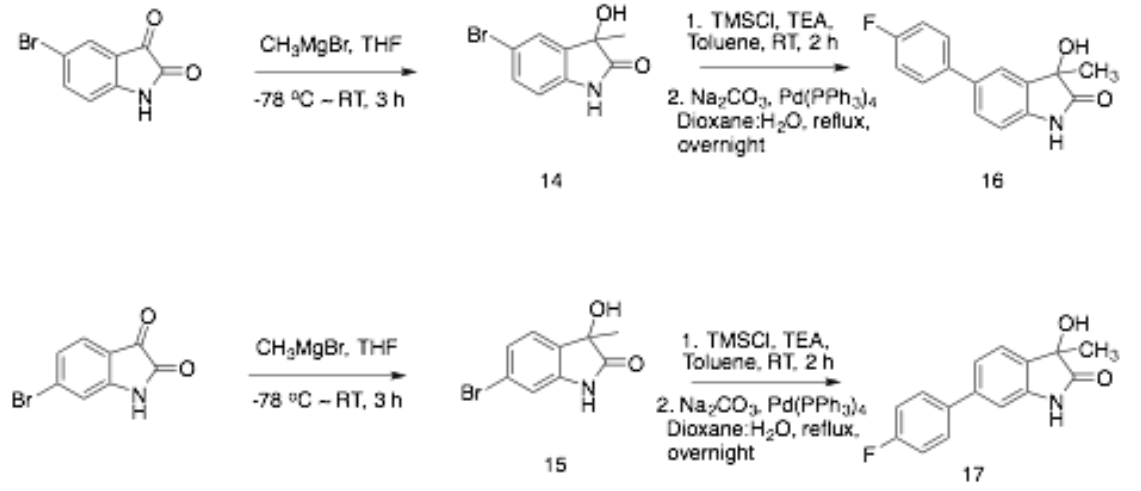

Scheme 17. Improvised synthesis of **16** and **17**

Testing of these compounds for endonuclease inhibition using a FRET based enzymatic assay showed sub-maximal inhibition at 200 μM. The percentage inhibition of each

molecule has been tabulated in Table 5. This can, however, be attributed to non-specific inhibition of the enzyme.

	Compound structure	Percent inhibition
14	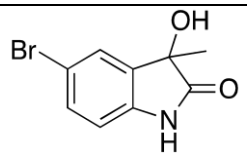	30% at 200 μM
15	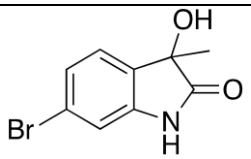	20% at 200 μM
16	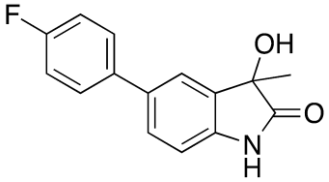	40% at 200 μM
17	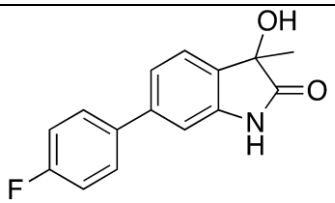	40% at 200 μM

Table 5. Biological activity of **14-17**

Also, a Grignard reaction using phenyl magnesium bromide was carried out on 5 and 6 substituted isatins to afford compounds **18-21** (Scheme 18**)** to study the effect of a bulkier substitution on the 3rd position. It was hypothesized that a bulky substituent like phenyl group would impart conformational rigidity at the 3-carbon causing better binding at the active site.

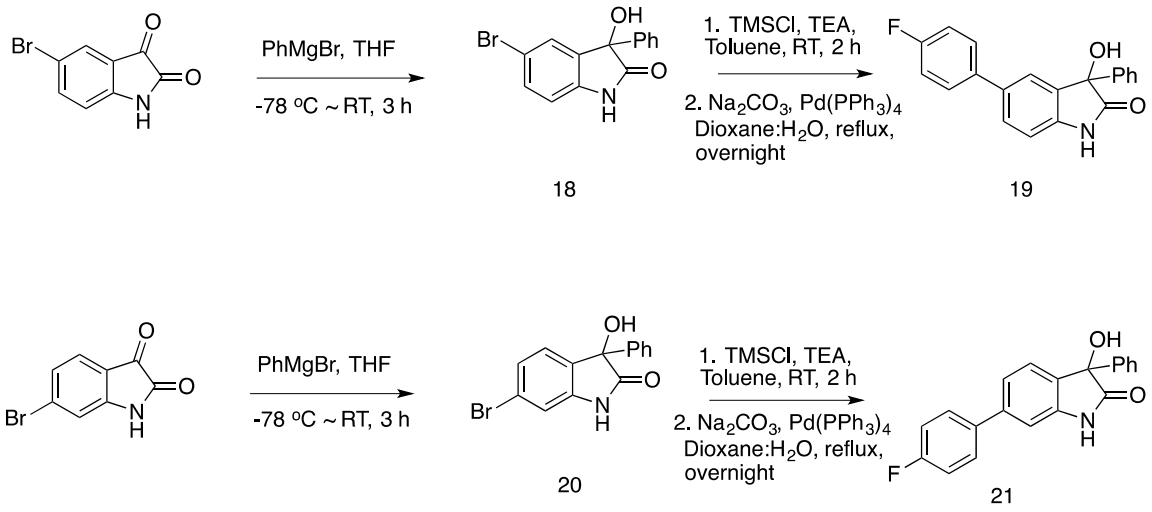

Scheme 18. Synthesis of **18-21**

However, none of these structural modifications resulted in better inhibitory activity than compounds **14-17** as seen in Table 6, suggesting that a bulky group at the 3rd position was not associated with enhanced activity.

	Compound Structure	IC_{50} (μM)
18	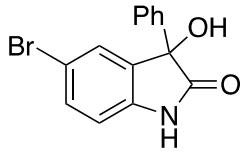	>600
19	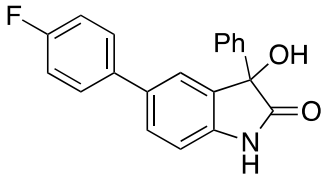	>600
20	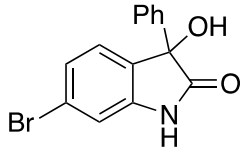	>600
21	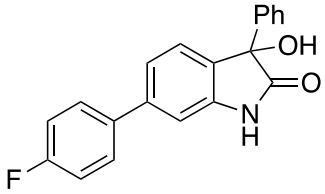	>600

Table 6. Biological activity of **18-21**

The last structural modification we explored to potentially improve the binding of the compounds at the endonuclease active site was addition of another chelating moiety. Hence, synthesis of N-hydroxy isatin was pursued. Introduction of N-hydroxy was at first pursued using oxidants like hydrogen peroxide or mCPBA on isatin.[21,22] These did not give the desired products (Scheme 19).

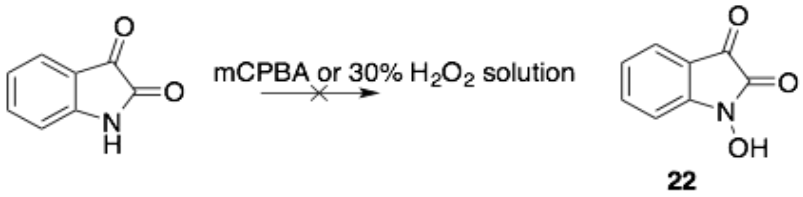

Scheme 19. Attempted synthesis I of **22**

We investigated an alternative approach which involved the construction of the heterocyclic portion of the isatin ring.[23] Acid chloride of 2-nitro benzoic acid was treated with TMS Diazomethane in basic conditions to give a diazoketone. This was then cyclized using formic acid and sulfuric acid to give N-hydroxy isatin, **22** (Scheme 20). The nitro group on the ring is involved in this unique cyclisation mechanism with loss of nitrogen gas.

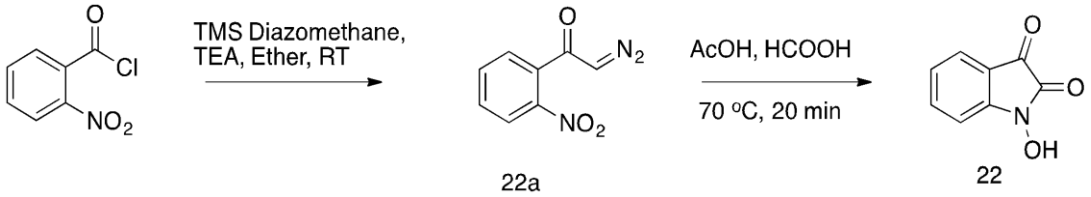

Scheme 20. Synthesis of **22**

In our *in vitro* assay, **22** showed 45% inhibition at 200 uM upon testing using the FRET assay as shown in Table 7. In the hope that further structural modification would result in better activity, the final series of compounds consisted of all essential pharmacophores; the 2-carbonyl, 1-hydroxy, 3-hydroxy and the hydrophobic 4-fluorophenyl group projecting from the 6-position of the substituted isatin. Synthesis of **23** was conducted in the same fashion as compound **22**. Formation of acid chloride **23b** from the acid **23a** using oxalyl chloride did not result in complete conversion and a substantial amount of acid remained. Similar observation was recorded when thionyl chloride was used despite being a stronger chlorinating agent. This was attributed to

interference of electronegative bromo substitution *para* to the acid moiety. The presence of the acid also interfered with formation of the diazoketone resulting in low yields of the diazoketone. This scheme of synthesis was pursued nevertheless, as the chlorine from acid chloride **23b** makes a good leaving group compared to other reported leaving groups like carbonates. Synthesis of **24** from **23** using methyl magnesium bromide (3.0 eq) was straightforward. Compound **25** was formed using *in-situ* TMS protection and subsequent Suzuki coupling. All of the aforementioned reactions for synthesis of **23-25** have been illustrated in Scheme 21.

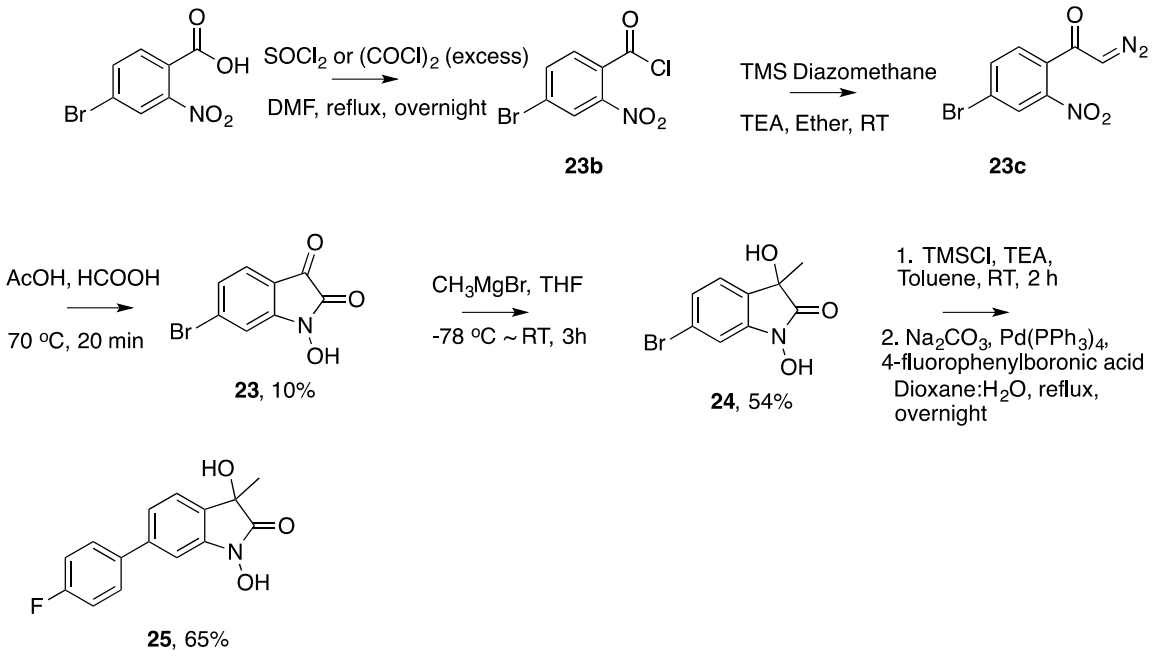

Scheme 21. Synthesis of **23-25**

Compounds **23-25** upon testing were found out to be inactive. Enzymatic assay results for **23-25** have been tabulated in Table 7. It was hypothesized that the geometry of chelating oxygens was not allowing for sufficient metal binding at the endonuclease active site, resulting in poor activity.

	Compound Structure	IC_{50} (μM)
22	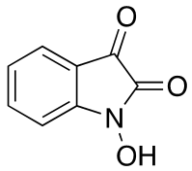	45% at 200
23	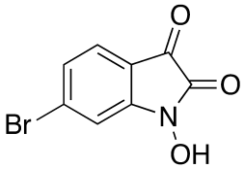	>600
24	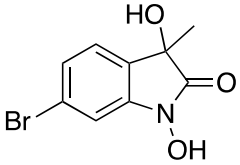	>600
25	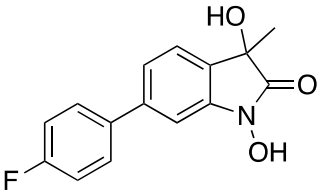	>600

Table 7. Biological activity of **22-25**

SUMMARY

There is a need to develop novel antiviral agents in view of the threat of the emergence of influenza pandemics. PA_N endonuclease is an interesting target owing to the fact that it is a highly conserved protein. PA_N, a subunit of RdRp houses endonuclease that catalyzes transcription by mediating the cap-snatching mechanism. Extensive studies led to development of three promising series of small molecules, 3-hydroxypyridin-2(1*H*)-ones, 3-hydroxyquinolin-2(1*H*)-ones and aza analogs of 3-hydroxypyridin-2(1*H*)-one with appreciable *in vitro* activity according to enzymatic FRET based assay. However, there was failure in translating these results to *ex vivo* activity in cellular assays. We hypothesized that usage of a truncated endonuclease instead of the whole RNP complex was providing misleading results. Compound **4**, a Shionogi patented compound[17], was synthesized as a means to explore this hypothesis.

We also investigated a new series of isatin based molecules which was developed based on SAR studies derived from 3-hydroxypyridin-2(1*H*)-ones. All molecules were ineffective as endonuclease inhibitors according to FRET-based assays. Compounds **16**, **17** and **22** showed marginal inhibition at 200 μM. The functional groups used in these compounds were combined to develop **25**. However, it was found to be inactive *in vitro.* The activity observed with **16**, **17** and **22** was attributed to non-specific inhibition. In conclusion, this dissertation elaborates the synthesis, SAR and biological studies of potential PA_N endonuclease inhibitors. In spite of lack of activity of the isatin series, continual research is being carried out in the hope of designing a novel, efficient anti-influenza drug that can be commercially developed in the future.

EXPERIMENTAL

General

Reactions were monitered using aluminum baked silica G TLC plates (Sorbent Technologies) with UV254 and visualized under ultraviolet light. Purification was done using Combi Flash Rf Teledyne ISCO flash chromatography system with 230-400 mesh silica gel columns (Teledyne ISCO). Solvents ethyl acetate (EtOAc), hexane, methanol (MeOH) or dichloromethane (CH_2Cl_2) were purchased from Sigma-Aldrich, Inc., USA and used as indicated in each procedure. NMR spectra, both proton ^{1}H (400 MHz) and carbon ^{13}C (100 MHz), were recorded using Bruker Avance III (400 MHz) Multinuclear NMR Spectrometer. Deuterated solvents ($CDCl_3$, DMSO-d_6) were purchased from Cambridge Isotopes Laboratory (Cambridge, MA). Chemical shift data was expressed in parts per million (δ) relative to residual nondeuterated solvent signal. Spin multiplicities were abbreviated as s (singlet), d (doublet), dd (doublet of doublets), t (triplet), dt (doublet of triplets), td (triplet of doublets), q (quartet), sep (septet), m (multiplet), br s (broad singlet). Coupling constants were reported in Hertz (Hz). Melting points (uncorrected) were calculated using Mel-temp II apparatus. HRMS data were analyzed using LC-MS Velos-LTQ-Orbitrap at the Department of Proteomics, Rutgers University.

Shionogi Inc. Compound (Reference Example 107 in patent)[17]

3-(Benzyloxy)-2-methyl-4*H*-pyran-4-one (**4b**)

3-Hydroxy-2-methyl-4*H*-pyran-4-one (1.0 g, 7.93 mmol) was dissolved in dry DMF and of benzyl bromide (4.86 mL, 7.93 mmol) was added. The mixture was stirred at 80 °C for 15 minutes and then potassium carbonate (1.2 g, 7.93 mmol) was added. The reaction was

further stirred overnight. Reaction was diluted with ethyl acetate and washed with $NaHCO_3$ and brine. Organic layer was dried over Na_2SO_4 and solvent evaporated under reduced pressure to obtain 1.7 g (100%) of **4b** as brown oil. ^{1}H NMR (400 MHz) ($CDCl_3$) δ 7.50 (d, *J* = 1 Hz, 1H), 7.37 (m, 5H), 6.41 (d, *J* = 1 Hz, 1H), 5.30 (s, 2H), 2.14 (s, 3H); ^{13}C NMR (100 MHz) ($CDCl_3$) δ 174.7, 159.3, 153.6, 143.5, 136.7, 14.4.

3-(Benzyloxy)-4-oxo-4*H*-pyran-2-carbaldehyde (**4c**)

3-(Benzyloxy)-2-methyl-4*H*-pyran-4-one (1.35 g, 6.24 mmol) was dissolved in bromobenzene and selenium dioxide (4.16 g, 37.49 mmol) was added. This suspension was heated at 160 °C and stirred for 16 h. Mixture was filtered using celite with ethyl acetate as solvent. Filtrate was evaporated under reduced pressure and product purified on ISCO chromatograph (0-50 % ethyl acetate/ hexane) to obtain 882 mg (63%) of **4c** as brown oil. ^{1}H NMR (400 MHz) ($CDCl_3$) δ 9.89 (s, 1H), 7.76 (d, *J* = 1 Hz, 1H), 7.38 (m, 5H), 6.53 (d, *J* = 1 Hz, 1H), 5.53 (s, 2H); ^{13}C NMR (100 MHz) ($CDCl_3$) δ 182.5, 177.1, 154.3, 151.8, 149.3, 135.0, 129.2, 129.1, 128.8, 128.7, 128.6, 118.3, 60.4

3-(Benzyloxy)-4-oxo-4*H*-pyran-2-carboxylic acid (**4d**)

3-(Benzyloxy)-4-oxo-4*H*-pyran-2-carbaldehyde (390 mg, 1.69 mmol) was dissolved in acetone:water (1:1.5) mixture. Sodium chlorite (161 mg, 1.69 mmol) and sulfamic acid (231 mg, 2.38 mmol) was added to the solution and the reaction stirred at room temperature for 5 hours. The solvent was evaporated using reduced pressure. The remaining residue was washed with ethyl acetate and filtered to obtain 300 mg (72%) of **4d** as a white waxy

solid. ^{1}H NMR (400 MHz) (DMSO) δ 8.22 (d, *J* = 1 Hz, 1H), 7.79 (m, 5H), 6.56 (d, *J* = 1 Hz, 1H), 5.12 (s, 2H); ^{13}C NMR (100 MHz) (DMSO) δ 175.5, 160.8, 155.4, 148.8, 137.3, 136.7, 128.2, 128.1, 127.9, 127.6, 127.3, 116.9, 75.5.

3-(Benzyloxy)-4-oxo-1,4-dihydropyridine-2-carboxylic acid (**4e**)

3-(Benzyloxy)-4-oxo-4*H*-pyran-2-carboxylic acid (500 mg, 2.03 mmol) was dissolved in an excess of aqueous ammonia and the solution was stirred at room temperature overnight. Aqueous ammonia was evaporated using reduced pressure and pH adjusted to 4-5 using 2N HCl. Product precipitate is washed with ethyl acetate and filtered to obtain 395 mg (80%) of **4e** as a yellow waxy solid. ^{1}H NMR (400 MHz) (DMSO) δ 7.67 (d, *J* = 1 Hz, 1H), 7.48 (d, *J* = 2 Hz) 2H), 7.34 (m, 3H), 6.49 (d, *J* = 1 Hz, 1H), 5.08 (s, 2H); ^{13}C NMR (100 MHz) (DMSO) δ 174.5, 160.8, 155.4, 148.9, 137.4, 136.7, 128.1, 128.0, 127.9, 127.7, 127.3, 117.0, 75.6

3-(Benzyloxy)-*N*-isopropyl-4-oxo-1,4-dihydropyridine-2-carboxamide (**4f**)

3-(Benzyloxy)-4-oxo-1,4-dihydropyridine-2-carboxylic acid (335 mg, 1.36 mmol) was dissolved in dry DMF. WSC.HCl (341 mg, 1.78 mmol) and benzotriazole (177 mg, 1.36 mmol) was added and the mixture stirred for 10 minutes. Isopropylamine solution (0.24 mL, 33 wt % in ethanol) was further added and the reaction stirred for 2 hours. Water was added to the reaction mixture and extracted using chloroform. The organic layer was evaporated under reduced pressure and the resulting residue was purified using ISCO chromatograph (0-10% methanol/CH_2Cl_2) to obtain 211 mg (55%) of **4f** as an oil. ^{1}H NMR (400 MHz) ($CDCl_3$) δ 10.16 (brs, 1H), 8.21 (d, *J* = 1 Hz, 1H), 7.39 (m, 5H), 6.56 (d, *J* = 1

Hz, 1H), 5.53 (s, 2H), 4.03 (sep, *J* = 2 Hz, 1H), 0.95 (d, *J* = 2 Hz, 6H); ^{13}C NMR (100 MHz) ($CDCl_3$) δ 175.4, 159.6, 148.0, 139.9 136.3, 134.2, 129.2, 128.9, 128.8, 128.6, 128.5, 128.4, 118.5, 74.9, 42.1, 22.6.

1-Amino-3-(benzyloxy)-*N*-isopropyl-4-oxo-1,4-dihydropyridine-2-carboxamide (**4g**)

3-(benzyloxy)-*N*-isopropyl-4-oxo-1,4-dihydropyridine-2-carboxamide (3.63 mmol) was dissolved in dry DMF, potassium carbonate (1.66 g, 12 mmol) was added and this suspension was stirred for 5 minutes. To this suspension was added *o*-(2,4-dinitrophenyl) hydroxylamine (1.2 g, 6.01 mmol) and the mixture stirred for 3 hours. Upon completion, water was added and the reaction mixture extracted with chloroform. Solvent was evaporated under reduced pressure and product purified using ISCO chromatograph (0-10% methanol/CH_2Cl_2) to obtain 560 mg (52%) of **4g** as a yellow powder. ^{1}H NMR (400 MHz) ($CDCl_3$) δ 7.39 (d, *J* = 1 Hz, 1H), 7.28 (m, 5H), 6.27 (d, *J* = 1 Hz, 1H), 5.55 (s, 2H), 5.22 (brs, 2H), 3.98 (sep, *J* = 2 Hz, 1H), 0.97 (d, *J* = 2 Hz, 6H); ^{13}C NMR (100 MHz) ($CDCl_3$) δ 175.5, 159.5, 148.0, 136.3, 133.9, 129.2, 128.9, 128.8, 128.6, 128.5, 118.5, 75.0, 42.2, 21.9

5-(Benzyloxy)-3-isopropyl-2,3-dihydro-1*H*-pyrido[2,1-*f*][1,2,4]triazine-4,6-dione (**4h**)

1-Amino-3-(benzyloxy)-*N*-isopropyl-4-oxo-1,4-dihydropyridine-2-carboxamide (240 mg, 0.796 mmol) was dissolved in dry DMF. Paraformaldehyde (26 mg, 0.865 mmol) and 2-3 drops of acetic acid were added and the solution stirred at 110 °C for 4 hours. Solvent was removed using reduced pressure and residue purified on ISCO chromatograph (0-10% methanol/CH_2Cl_2) to obtain 190 mg (76%) of **4h** as a waxy solid. ^{1}H NMR (400 MHz)

($CDCl_3$) δ 7.55 (d, *J* = 1 Hz, 1H), 7.32 (m, 5H), 6.27 (d, *J* = 1 Hz, 1H), 5.95 (brt, 1H), 5.26 (s, 2H), 4.73 (sep, *J* = 2 Hz, 1H), 4.31 (d, *J* = 2 Hz, 2H) 1.17 (d, *J* = 2 Hz, 6H); ^{13}C NMR (100 MHz) ($CDCl_3$) δ 175.1, 155.1, 138.3, 137.0, 129.2, 128.1, 127.9, 116.2, 73.6, 55.9, 44.0, 19.8

5-(Benzyloxy)-1-(bis(2-chlorophenyl)methyl)-3-isopropyl-2,3-dihydro-1*H*-pyrido[2,1-*f*][1,2,4]triazine-4,6-dione (**4**)

5-(Benzyloxy)-3-isopropyl-2,3-dihydro-1*H*-pyrido[2,1-*f*][1,2,4]triazine-4,6-dione (242 mg, 0.77 mmol) was dissolved in acetic acid. 0.5 mL of 96% sulfuric acid and 585 mg of bis(2-chlorophenyl)methanol (2.31 mmol) were added to the solution. The reaction mixture was then stirred at 80 °C for 2 hours. The reaction mixture was extracted with ethyl acetate and purified on ISCO chromatograph (0-10% methanol/CH_2Cl_2) to obtain 40 mg (11%) of **4** as an orange solid. mp 241-243 °C; ^{1}H NMR (400 MHz) ($CDCl_3$) δ 8.00 (d, *J* = 2 Hz, 1H), 7.45 (t, *J* = 2 Hz, 1H), 7.32 (m, 2H), 7.10 (m, 5H), 6.64 (d, *J* = 2 Hz, 1H), 6.41 (s, 1H), 5.66 (d, *J* = 2 Hz, 1H), 4.87 (m, 1H), 4.42 (d, *J* = 12 Hz, 1H), 1.05 (d, *J* = 2 Hz, 3H), 0.98 (d, *J* = 2 Hz, 3H); ^{13}C NMR (100 MHz) ($CDCl_3$) δ 171.9, 161.4, 152.4, 136.8, 136.1, 135.9, 134.2, 132.1, 131.2, 130.8, 130.6, 130.4, 129.7, 127.8, 127.5, 126.9, 117.4, 111.3, 61.8, 59.3, 53.4, 43.7, 19.5, 18.8; HRMS calculated for $C_{23}H_{22}Cl_2N_3O_3$ $(M+H)^+$ 458.0994, found 458.1026.

Conversion of Isatin and Isatin Derivatives to 3-Hydroxy-indolin-2-ones

3-Hydroxyindolin-2-one (**5**)

Sodium borohydride (75.66 mg, 2.04 mmol) was suspended in CH_2Cl_2-ethanol (1:1) in a dry round bottom flask and indoline-2,3-dione (200 mg, 1.36 mmol) was added at 0 °C. The suspension was stirred for 5 minutes at the same temperature until it became colorless. The reaction was monitored using thin-layer chromatography (TLC). Water was added to the reaction mixture and it was stirred until bubbling stopped. The mixture was extracted with CH_2Cl_2. The organic layer was dried over sodium sulfate and solvent removed using reduced pressure to yield 101 mg (48%) of **5**. ^{1}H NMR (400 MHz) (DMSO) δ 10.42 (brs, 1H), 7.49 (d, *J* = 8 Hz, 1H), 7.41 (t, *J* = 8 Hz, 1H), 7.17 (t, *J* = 8 Hz, 1H), 6.99 (d, *J* = 8 Hz, 1H), 5.03 (d, *J* = 8 Hz, 1H).

4-Bromo-3-hydroxyindolin-2-one (**6**)

Sodium borohydride (50 mg, 1.32 mmol) was suspended in CH_2Cl_2-ethanol (1:1) in a dry round bottom flask and to it was added 4-bromoindoline-2,3-dione (200 mg, 0.88 mmol) at 0 °C. The suspension was stirred for 5 minutes at 0 °C until it became colorless. The reaction was monitored using thin-layer chromatography (TLC). Water was added to the reaction mixture and it was stirred until bubbling stopped. The mixture was extracted with CH_2Cl_2. The organic layer was dried over sodium sulfate and solvent removed using reduced pressure to yield 84 mg (42%) of product (**6**). ^{1}H NMR (400 MHz) (DMSO) δ 10.45 (brs, 1H), 7.16 (t, *J* = 8 Hz, 1H), 6.79 (d, *J* = 8 Hz, 1H), 6.24 (d, *J* = 8 Hz, 1H), 4.77 (d, *J* = 8 Hz, 1H).

5-Bromo-3-hydroxyindolin-2-one (**7**)

Sodium borohydride (50 mg, 1.32 mmol) was suspended in CH_2Cl_2-ethanol (1:1) in a dry round bottom flask and to it was added 5-bromoindoline-2,3-dione (200 mg, 0.88 mmol) at 0 °C. The suspension was stirred for 5 minutes at 0 °C until it became colorless. The reaction was monitored using thin-layer chromatography (TLC). Water was added to the reaction mixture and it was stirred until bubbling stopped. The mixture was extracted with CH_2Cl_2. The organic layer was dried over sodium sulfate and solvent removed using reduced pressure to yield 120 mg (60%) of product (**7**). ^{1}H NMR (400 MHz) (DMSO) δ 10.41 (brs, 1H), 7.45 (s, 1H), 6.81 (d, *J* = 8 Hz, 1H), 6.31 (d, *J* = 8 Hz, 1H), 4.93 (d, *J* = 8 Hz, 1H).

6-Bromo-3-hydroxyindolin-2-one (**8**)

Sodium borohydride (50 mg, 1.32 mmol) was suspended in CH_2Cl_2-ethanol (1:1) in a dry round bottom flask and to it was added 6-bromoindoline-2,3-dione (200 mg, 0.88 mmol) at 0 °C The suspension was stirred for 5 minutes at 0 °C until it became colorless. The reaction was monitored using thin-layer chromatography (TLC). Water was added to the reaction mixture and it was stirred until bubbling stopped. The mixture was extracted with CH_2Cl_2. The organic layer was dried over sodium sulfate and solvent removed using reduced pressure to yield 90 mg (45%) of product (**8**). ^{1}H NMR (400 MHz) (DMSO) δ 10.42 (brs, 1H), 7.44 (s, 1H), 7.25 (d, *J* = 8 Hz, 1H), 6.40 (d, *J* = 8 Hz, 1H), 4.84 (d, *J* = 8 Hz, 1H).

7-Bromo-3-hydroxyindolin-2-one (**9**)

Sodium borohydride (50 mg, 1.32 mmol) was suspended in CH_2Cl_2-ethanol (1:1) in a dry round bottom flask and to it was added 7-bromoindoline-2,3-dione (200 mg, 0.88 mmol) at 0 °C The suspension was stirred for 5 minutes at 0 °C until it became colorless. The reaction was monitored using thin-layer chromatography (TLC). Water was added to the reaction mixture and it was stirred until bubbling stopped. The mixture was extracted with CH_2Cl_2. The organic layer was dried over sodium sulfate and solvent removed using reduced pressure to yield 112 mg (56%) of product (**9**). ^{1}H NMR (400 MHz) (DMSO) δ 7.40 (d, *J* = 8 Hz, 1H), 7.28 (d, *J* = 8 Hz, 1H), 6.93 (t, *J* = 8 Hz, 1H), 6.30 (d, *J* = 8 Hz, 1H), 4.95 (d, *J* = 8 Hz, 1H).

Suzuki Couplings with Bromoindoline-2,3-diones

4-(4-Fluorophenyl)indoline-2,3-dione (**10**)

A dry round bottom flask was purged with nitrogen. 4-bromoindoline-2,3-dione (200 mg, 0.88 mmol) was dissolved in dioxane:water (3:1). To this solution, 4-fluorophenyl boronic acid (166 mg, 1.18 mmol), sodium carbonate (280 mg, 2.6 mmol, 3.0 eq) and tetrakis(triphenylphosphine)palladium(0) (40 mg, 0.03 mmol) was added. The mixture was stirred under inert atmosphere at reflux, overnight. After monitoring with TLC, mixture was diluted with ethyl acetate and washed using saturated ammonium chloride, followed by brine. The organic layer was dried with sodium sulfate, filtered and evaporated under reduced pressure. Crude product was purified using ISCO (30% ethyl

acetate/hexanes) to give 25 mg (10%) of white powder. mp 79-81 °C; ^{1}H NMR (400 MHz) (DMSO) δ 7.37-7.44 (m, 2H), 7.20-7.22 (m, 3H), 7.00-7.06 (m, 2H); ^{13}C NMR (100 MHz) (DMSO) δ 163.0, 160.6, 136.6, 136.5, 133.3, 133.1, 128.9, 128.7, 128.7, 128.6, 128.5, 115.8, 115.5.

5-(4-Fluorophenyl)indoline-2,3-dione (**11**)

A dry round bottom flask was purged with nitrogen. 5-bromoindoline-2,3-dione (200 mg, 0.88 mmol) was dissolved in dioxane:water (3:1). To this solution, 4-fluorophenyl boronic acid (166 mg, 1.18 mmol), sodium carbonate (280 mg, 2.6 mmol, 3.0 eq) and tetrakis(triphenylphosphine)palladium(0) (40 mg, 0.03 mmol) was added. The mixture was stirred under inert atmosphere at reflux, overnight. After monitoring with TLC, mixture was diluted with ethyl acetate and washed using saturated ammonium chloride, followed by brine. The organic layer was dried with sodium sulfate, filtered and evaporated under reduced pressure. Crude product was purified using ISCO (30% ethyl acetate in hexanes) to give 104 mg (43%) of white powder. mp 79-81 °C; ^{1}H NMR (400 MHz) (DMSO) δ 7.56-7.59 (m, 2H), 7.50-7.53 (m, 2H), 7.46 (t, J = 8 Hz, 1H), 7.11-7.17 (m, 2H); ^{13}C NMR (100 MHz) (DMSO) δ 163.0, 160.6, 139.1, 136.6, 136.6, 135.6, 135.6, 128.9, 128.6, 128.5, 127.3, 126.6, 115.7, 115.5.

6-(4-Fluorophenyl)indoline-2,3-dione (**12**)

A dry round bottom flask was purged with nitrogen. 6-bromoindoline-2,3-dione (200 mg, 0.88 mmol) was dissolved in dioxane:water (3:1). To this solution, 4-fluorophenyl boronic

acid (166 mg, 1.18 mmol), sodium carbonate (280 mg, 2.6 mmol, 3.0 eq) and tetrakis(triphenylphosphine)palladium(0) (40 mg, 0.03 mmol) was added. The mixture was stirred under inert atmosphere at reflux, overnight. After monitoring with TLC, mixture was diluted with ethyl acetate and washed using saturated ammonium chloride, followed by brine. The organic layer was dried with sodium sulfate, filtered and evaporated under reduced pressure. Crude product was purified using ISCO (30% Ethyl acetate/hexanes) to give 29 mg (12%) of white powder. mp 80-82 °C ; ^{1}H NMR (400 MHz) (DMSO) δ 7.57-7.60 (m, 2H), 7.50-7.53 (m, 2H), 7.46 (t, *J* = 8 Hz, 1H), 7.11-7.17 (m, 2H); ^{13}C NMR (100 MHz) (DMSO) δ 163.0, 160.6, 139.1, 136.6, 136.6, 135.6, 135.6, 128.9, 128.7, 127.4, 126.6, 115.8, 115.6.

7-(4-Fluorophenyl)indoline-2,3-dione (**13**)

A dry round bottom flask was purged with nitrogen. 7-bromoindoline-2,3-dione (200 mg, 0.88 mmol) was dissolved in dioxane:water (3:1). To this solution, 4-fluorophenyl boronic acid (166 mg, 1.18 mmol), sodium carbonate (280 mg, 2.6 mmol, 3.0 eq) and tetrakis(triphenylphosphine)palladium(0) (40 mg, 0.03 mmol) was added. The mixture was stirred under inert atmosphere at reflux, overnight. After monitoring with TLC, mixture was diluted with ethyl acetate and washed using saturated ammonium chloride, followed by brine. The organic layer was dried with sodium sulfate, filtered and evaporated under reduced pressure. Crude product was purified using ISCO (30% Ethyl acetate/hexanes) to give 109 mg (45%) of white powder. mp 81-83 °C; ^{1}H NMR (400 MHz) (DMSO) δ 7.38-7.43 (m, 2H), 7.21-7.26 (m, 3H), 7.00-7.06 (m, 2H); ^{13}C NMR (100

MHz) (DMSO) δ 163.0, 160.6, 139.1, 136.6, 136.6, 135.6, 135.6, 128.9, 128.6, 128.5, 127.3, 126.6, 115.7, 115.5.

Methyl Grignard Reactions with 6-Bromoindoline-2,3-diones

5-Bromo-3-hydroxy-3-methylindolin-2-one (**14**)

6-Bromoindoline-2,3-dione (1.0 g, 4.4 mmol) was dissolved in THF in a dry round bottom flask and the solution was cooled to 0 °C. Methyl magnesium bromide (1.5 mL, 13.2 mmol) was added and the reaction was warmed to room temperature and stirred overnight. Upon completion, the reaction was quenched with saturated ammonium chloride and extracted using ethyl acetate. The organic layer was dried over sodium sulfate and evaporated under reduced pressure. Crude product was purified using an ISCO to obtain 326 mg (31%) of **14**. ^{1}H NMR (400 MHz) ($CDCl_3$) δ 10.36 (brs, 1H), 7.44 (s, 1H), 7.37 (d, *J* = 8 Hz, 1H), 6.77 (d, 8 Hz, 1H), 5.99 (s, 1H), 1.36 (s, 3H); ^{13}C NMR (100 MHz) ($CDCl_3$) δ 179.1, 140.3, 136.0, 131.3, 126.3, 113.3, 111.5, 72.6, 24.1.

6-Bromo-3-hydroxy-3-methylindolin-2-one (**15**)

6-bromoindoline-2,3-dione (1.0 g, 4.4 mmol) was dissolved in THF in a dry round bottom flask and the solution was cooled to 0 °C. Methyl magnesium bromide (1.5 mL, 13.2 mmol) was added and the reaction was warmed to room temperature and stirred overnight Upon completion, the reaction was quenched with saturated ammonium chloride and extracted using ethyl acetate. The organic layer was dried over sodium sulfate and evaporated under reduced pressure. Crude product was purified using an ISCO (50% ethyl acetate/hexanes) to obtain 823 mg (77%) of **15**. mp 191-193 °C; ^{1}H NMR (400 MHz) ($CDCl_3$) δ 11.14 (s,

1H), 7.45 (d, *J* = 8 Hz, 1H), 7.27 (d, *J* = 8 Hz, 1H), 7.09 (s, 1H), 1.35 (s, 3H); ^{13}C NMR (100 MHz) ($CDCl_3$) δ 179.3, 142.8, 132.8, 125.2, 124.1, 121.2, 114.9, 112.3, 72.2, 24.1.

Suzuki Couplings with 5-Bromo-3-hydroxy-3-methylindolin-2-ones

5-(4-Fluorophenyl)indoline-2,3-dione (**16**)

5-bromo-3-hydroxy-3-methylindolin-2-one (**14**) (100 mg, 0.41 mmol) was dissolved in toluene in a dry round bottom flask. Trimethyl silyl chloride (178 mg, 1.64 mmol) and triethylamine (0.11 mL, 0.82 mmol) was added to the solution and the mixture was stirred at room temperature for 4 hours. Toluene was removed under reduced pressure. Crude product from this reaction was dissolved in dioxane:water (2:1). 4-fluorophenyl boronic acid (228 mg, 1.64 mmol) and sodium carbonate (130 mg, 1.23 mmol) was added. Air in the round bottom flask was replaced with nitrogen and tetrakis(triphenylphosphine)palladium(0) (46 mg, 0.016 mmol) was added. The mixture was stirred at reflux overnight. Mixture was diluted with ethyl acetate and washed with water, followed by brine. Organic layer was dried over sodium sulfate, filtered and solvent was evaporated using reduced pressure. Purification by ISCO (60% ethyl acetate in hexanes) afforded 80 mg (76%) of **16**. mp 224-226 °C; ^{1}H NMR (400 MHz) (DMSO) δ 10.32 (brs, 1H), 7.64-7.68 (m, 2H), 7.58 (s, 1H), 7.50 (dd, *J* = 8, 4 Hz, 1H), 7.27 (t, *J* = 12 Hz, 2 H), 6.90 (d, *J* = 8 Hz, 1H), 5.93 (s, 1H), 1.43 (s, 3H); ^{13}C NMR (100 MHz) (DMSO) δ 184.9, 167.9, 165.4, 145.8, 141.9, 139.6, 138.1, 133.3, 133.2, 127.0, 120.9, 115.1, 77.9, 29.6; HRMS data calculated for $C_{15}H_{11}FNO_1$ (M^+-OH) 240.0833, found (M^+-OH) 240.0818.

6-(4-Fluorophenyl)indoline-2,3-dione (**17**)

5-Bromo-3-hydroxy-3-methylindolin-2-one (**14**) (100 mg, 0.41 mmol) was dissolved in toluene in a dry round bottom flask. Trimethyl silyl chloride (178 mg, 1.64 mmol) and triethylamine (0.11 mL, 0.82 mmol) was added to the solution and the mixture was stirred at room temperature for 4 hours. Toluene was removed under reduced pressure. Crude product from this reaction was dissolved in dioxane:water (2:1). 4-fluorophenyl boronic acid (228 mg, 1.64 mmol) and sodium carbonate (130 mg, 1.23 mmol) was added. Air in the round bottom flask was replaced with nitrogen and tetrakis(triphenylphosphine)palladium(0) (46 mg, 0.016 mmol) was added. The mixture was stirred at reflux overnight. Mixture was diluted with ethyl acetate and washed with water, followed by brine. Organic layer was dried over sodium sulfate, filtered and solvent was evaporated using reduced pressure. Purification by ISCO (60% ethyl acetate in hexanes) afforded 51 mg (48%) of **17**. 201-202 °C dec; ^{1}H NMR (400 MHz) (DMSO) δ 10.32 (brs, 1H), 7.61-7.68 (m, 2H), 7.35 (d, *J* = 8 Hz, 1H), 7.27 (t, *J* = 8 Hz, 2H), 7.20 (d, *J* = 8 Hz, 1H), 6.96 (s, 1H), 5.88 (s, 1H), 1.37 (s, 3H); ^{13}C NMR (100 MHz) (DMSO) δ 179.7, 163.0, 160.6, 141.8, 140.0, 136.7, 132.7, 128.7, 128.6, 123.8, 120.2, 115.7, 107.8, 72.4, 24.3; HRMS data calculated for $C_{15}H_{11}FNO_1$ (M^+-OH) 240.0833, found (M^+-OH) 240.0820.

Phenyl Grignard with Bromo substituted indoline-2,3-diones

5-Bromo-3-hydroxy-3-phenylindolin-2-one (**18**)

5-Bromoindoline-2,3-dione (1.0 g, 4.4 mmol) was dissolved in THF in a dry round bottom flask and the solution was cooled to 0 °C. Phenyl magnesium bromide (1.4 mL of a 6.2 M solution in THF, 8.8 mmol) was added and the reaction was warmed to room temperature and stirred overnight. Upon completion, the reaction was quenched with saturated ammonium chloride and extracted using ethyl acetate as the organic solvent. The organic layer was dried over sodium sulfate and evaporated using reduced pressure. Crude product was purified using an ISCO to obtain 320 mg (24%) of **18**. mp 229-231 °C; ^{1}H NMR (400 MHz) (DMSO) δ 10.57 (brs, 1H), 7.45 (d, *J* = 12 Hz, 1H), 7.28-7.34 (m, 5H), 7.21 (s, 1H), 6.88 (d, *J* = 8 Hz, 1H), 6.78 (brs, 1H); ^{13}C NMR (100 MHz) (DMSO) δ 177.9, 141.2, 140.7, 136.0, 131.9, 128.2, 127.6, 127.3, 125.2, 113.5, 111.9, 77.2; HRMS data calculated for $C_{14}H_9BrNO_1$ (M^+-OH) 285.9868, found (M^+-OH) 285.9865.

6-Bromo-3-hydroxy-3-phenylindolin-2-one (**20**)

6-Bromoindoline-2,3-dione (1.0 g, 4.4 mmol) was dissolved in THF in a dry round bottom flask and the solution was cooled to 0 °C. Phenyl magnesium bromide (1.4 mL of a 6.2 M solution in THF, 8.8 mmol) was added and the reaction was warmed to room temperature and stirred overnight. Upon completion, the reaction was quenched with saturated ammonium chloride and extracted using ethyl acetate as the organic solvent. The organic layer was dried over sodium sulfate and evaporated using reduced pressure. Crude product was purified using an ISCO (50% ethyl acetate in hexanes) to obtain 186 mg (14%) of **20**. mp 212-214 °C; ^{1}H NMR (400 MHz) (DMSO) δ 10.55 (brs, 1H), 7.30 (m, 5H), 7.16, (d, *J*

= 8 Hz, 1H), 7.04 (d, *J* = 8 Hz, 2H), 6.72 (s, 1H); ^{13}C NMR (100 MHz) (DMSO) δ 178.1, 143.6, 140.8, 132.9, 128.1, 127.5, 126.5, 125.3, 124.6, 121.7, 112.6, 76.9; HRMS data calculated for $C_{14}H_9BrNO_{11}$ (M^+-OH) 285.9868, found (M^+-OH) 285.9867.

Suzuki Couplings with Bromo-substituted 3-hydroxy-3-phenylindolin-2-ones

5-(4-Fluorophenyl)-3-hydroxy-3-phenylindolin-2-one (**19**)

5-Bromo-3-hydroxy-3-phenylindolin-2-one (**18**) (160 mg, 0.50 mmol) was dissolved in toluene in a dry round bottom flask. Trimethyl silyl chloride (287 mg, 2.64 mmol) and triethylamine (0.2 mL, 1.32 mmol) was added to the solution and the mixture was stirred at room temperature for 4 hours. Toluene was removed using reduced pressure. Crude product from this reaction was dissolved in dioxane:water (2:1). 4-Fluorophenyl boronic acid (370 mg, 2.64 mmol) and 210 mg of sodium carbonate (1.98 mmol) was added. Air in the round bottom flask was replaced with nitrogen and tetrakis(triphenylphosphine)palladium(0) (35 mg, 0.03 mmol) was added. The mixture was stirred at reflux overnight. Mixture was diluted with ethyl acetate and washed with water, followed by brine. Organic layer was dried over sodium sulfate, filtered and solvent was evaporated using reduced pressure. Purification by ISCO (60% ethyl acetate in hexanes) afforded 89 mg (42%) of **19**. mp 208-210 °C; ^{1}H NMR (400 MHz) (DMSO) δ 10.50 (brs, 1H), 7.56-7.60 (m, 2H), 7.33-7.35 (m, 5H), 7.20-7.30, 4H), 7.00 (d, *J* = 8 Hz, 1H), 6.69 (s, 1H), 5.76 (s, 1H); ^{13}C NMR (100 MHz) DMSO) δ 178.5, 141.3, 141.2, 136.3, 134.4, 133.5, 133.3, 129.2, 128.1, 128.0, 128.0, 127.9, 127.6, 127.5, 127.4, 125.3, 124.6, 122.8, 115.7, 115.5, 110.4, 77.3; HRMS data calculated for $C_{20}H_{13}FNO_1$ (M^+-OH) 302.0981, found (M^+-OH) 302.097

6-(4-Fluorophenyl)-3-hydroxy-3-phenylindolin-2-one (**21**)

6-bromo-3-hydroxy-3-phenylindolin-2-one (**20**) (93 mg, 0.30 mmol) was dissolved in toluene in a dry round bottom flask. Trimethyl silyl chloride (165 mg, 1.52 mmol) and triethylamine (0.1 mL, 0.76 mmol) was added to the solution and the mixture was stirred at room temperature for 4 hours. Toluene was removed using reduced pressure. Crude product from this reaction was dissolved in dioxane:water (2:1). 4-Fluorophenyl boronic acid (213 mg, 1.52 mmol) and sodium carbonate (121 mg, 1.14 mmol) was added. Air in the round bottom flask was replaced with nitrogen and tetrakis(triphenylphosphine)palladium(0) (17 mg, 0.015 mmol) was added. The mixture was stirred at reflux overnight. Mixture was diluted with ethyl acetate and washed with water, followed by brine. Organic layer was dried over sodium sulfate, filtered and solvent was evaporated using reduced pressure. Purification using an ISCO (60% ethyl acetate in hexanes) afforded 89 mg (93%) of **21**. mp 234-235 °C; ^{1}H NMR (400 MHz) (DMSO) δ 7.49-7.56 (m, 4H), 7.37-7.40 (m, 2H), 7.35 (s, 1H), 7.25 (d, *J* = 1.6 Hz, 2H), 7.12-7.18 (m, 3H); ^{13}C NMR (100 MHz) (DMSO) δ 178.5, 163.1, 142.6, 141.3, 140.4, 136.6, 132.8, 128.7, 128.6, 128.0, 127.4, 125.4, 125.1, 120.6, 115.8, 115.6, 115.6, 108.0, 77.1; HRMS data calculated for $C_{20}H_{13}FNO_1$ (M^+-OH) 302.0981, found (M^+-OH) 302.0974.

1-Hydroxyindoline-2,3-dione (**22**)

Triethylamine (0.7 mL, 5.94 mmol) was added to diethyl ether in a dry round bottom flask and the solution was cooled to 0 °C. 2.0 M solution of TMS diazomethane (2.9 mL, 678 mg, 5.94 mmol) was added to the solution. 2-Nitrobenzoyl chloride (1.0 g, 5.4 mmol) was added to the solution and it was stirred until product was detected by TLC. After reaction

reached completion, the mixture was filtered to remove insoluble by-product and the filtrate contained the crude product. The organic layer from filtrate was evaporated using reduced pressure and 150 mg of crude **22a** was taken and used in the next step. 150 mg of 2-diazo-1-(2-nitrophenyl)ethan-1-one (**22a**) (0.78 mmol) was dissolved in 1.5 mL of acetic acid and 0.1 mL of formic acid (catalytic) was added. The solution was stirred at 70 °C for 15-20 minutes until red crystals were observed. The mixture was cooled and the crystals were filtered using ether to obtain 40 mg (31%) of **22**. mp 234-235 °C; ^{1}H NMR (400 MHz) ($CDCl_3$) δ 11.14 (s, 1H), 7.66 (td, *J* = 8, 4 Hz, 1H) 7.52 (d, *J* = 8 Hz, 1H), 7.13 (td, *J* = 8, 0.8 Hz, 1H), 7.06 (d, *J* = 8 Hz, 1H); ^{13}C NMR (100 MHz) ($CDCl_3$) δ 181.2, 153.8, 149.3, 138.0, 123.7, 123.4, 116.3, 108.8.

1-(4-Bromo-2-nitrophenyl)-2-diazoethan-1-one (**23b**)

4-Bromo-2-nitrobenzoic acid (2.0 g, 8.13 mmol) was dissolved in CH_2Cl_2 in a dry round bottom flask and an excess of oxalyl chloride (3 mL) was added. Catalytic amounts of anhydrous DMF (2-3 drops) was added and the suspension was stirred for 4 hours. Oxalyl chloride was removed by washing with CH_2Cl_2 and then evaporating under reduced pressure. Crude product **23b** was then dissolved in ether. Triethylamine (2.8 mL, 19.66 mmol) and TMS diazomethane (3.0 mL,19.66 mmol) was added to ether in another dry round bottom flask. To this solution was added **23b** in ether and the mixture was stirred at room temperature overnight. The organic layer from filtrate was evaporated using reduced pressure and crude **23c** was used in the next step.

6-Bromo-1-hydroxyindoline-2,3-dione (**23**)

1-(4-Bromo-2-nitrophenyl)-2-diazoethan-1-one (23b) (500 mg, 1.85 mmol) was dissolved in 1.5 mL acetic acid in a dry round bottom flask and 0.1 mL of formic acid (catalytic) was added. The solution was stirred at 70 °C for 15-20 minutes until red crystals were observed. The mixture was cooled and the crystals were filtered using ether to obtain 44 mg (10%) of **23**. ^{1}H NMR (400 MHz) (DMSO) δ 11.25 (brs, 1H), 7.43 (d, *J* = 8 Hz, 1H), 7.31 (dd, *J* = 8, 1.6 Hz, 1H), 7.21 (d, *J* = 2 Hz, 1H); ^{13}C NMR (100 MHz) (DMSO) δ 131.9, 131.3, 126.1, 125.2, 122.1, 117.7, 115.5, 111.7.

6-Bromo-1,3-dihydroxy-3-methylindolin-2-one (**24**)

6-Bromo-1-hydroxyindoline-2,3-dione (23) (44 mg, 0.18 mmol) was dissolved in anhydrous THF in a dry round bottom flask. The solution was cooled to 0 °C and methyl magnesium bromide (0.17 mL, 0.54 mmol) was added. The solution was stirred at room temperature for 3 hours. Upon completion, the reaction was quenched with saturated ammonium chloride and extracted with ethyl acetate. The organic layer was dried over sodium sulfate and evaporated under reduced pressure. Crude product was purified using ISCO (50% ethyl acetate/hexanes) to obtain 25 mg (54%) of **24**. ^{1}H NMR (400 MHz) ($CDCl_3$) δ 7.01 (s, 1H), 7.19 (d, *J* = 1.7 Hz, 1H), 7.25 (d, *J* = 7.8 Hz, 1H); ^{13}C NMR (100 MHz) ($CDCl_3$) δ 172.9, 143.4, 129.5, 124.8, 124.7, 121.5, 109.8, 70.9

6-(4-Fluorophenyl)-1,3-dihydroxy-3-methylindolin-2-one (**25**)

6-Bromo-1,3-dihydroxy-3-methylindolin-2-one (**24**) (61 mg, 0.23 mmol) was dissolved in toluene in a dry round bottom flask. Trimethyl silyl chloride (0.12 mL, 0.92 mmol) and triethylamine (0.06 mL, 0.46 mmol) was added to the solution and the mixture was stirred at room temperature for 4 hours. Toluene was removed under reduced pressure. Crude product from this reaction was dissolved in dioxane:water (2:1). 4-Fluorophenyl boronic acid (129 mg, 0.92 mmol) and sodium carbonate (73 mg, 0.69 mmol) was added. Air in the round bottom flask was replaced with nitrogen and tetrakis(triphenylphosphine)palladium(0) (10 mg, 0.01 mmol) was added. The mixture was stirred at reflux overnight. Mixture was diluted with ethyl acetate and washed with water, followed by brine. The organic layer was dried over sodium sulfate, filtered and solvent was evaporated using reduced pressure. Purification using an ISCO (60% ethyl acetate in hexanes) afforded 40 mg (65%) of **25**. mp 232-234 °C; ^{1}H NMR (400 MHz) ($CDCl_3$) δ 10.28 (brs, 1H), 7.61 (t, *J* = 8 Hz, 2H), 7.33 (d, *J* = 8 Hz, 1H), 7.25 (t, *J* = 8 Hz, 2H), 7.18 (d, *J* = 8 Hz, 1H), 6.95 (s, 1H), 5.85 (s, 1H), 1.36 (s, 3H); ^{13}C NMR (100 MHz) ($CDCl_3$) δ 179.7, 163.0, 160.6, 141.8, 140.0, 136.8, 132.7, 128.6, 123.8, 120.2, 115.7, 107.8, 72.4, 54.8, 24.3; HRMS data calculated for $C_{15}H_{11}FNO_1$ (M^{+1}-H_2O_2) 240.0825, found (M^{+1}-H_2O_2) 240.0819.

REFERENCES

1. WHO. Influenza (seasonal). Fact sheet; March, 2014. http://www.who.int/mediacentre/factsheets/fs211/en/index.html.

2. Lüscher-Mattli, M. Influenza chemotherapy: a review of the present state of art and of new drugs in development. *Arch. Virol.* **2000**, *145*, 2233-2248.

3. Das, K.; Aramini, J. M.; Ma, L.-C.; Krug, R. M.; Arnold, E. Structures of influenza A proteins and insights into antiviral drug targets. *Nature Struct. Mol. Biol.*, **2010**, *17*, 530-538.

4. Stiver G. The treatment of influenza with antiviral drugs. *CMAJ: Canadian Medical Association Journal*. 2003;168(1):49-57.

5. Bright, R. A.; Medina, M.; Xu, X.; Peresz-Oronoz, G.; Wallis, T. R.; Davis, X. M.; Provinelli, L.; Cox, N. J.; Klimov, A. I. Incidence of admantane resistance among influenza A (H3N2) viruses isolated worldwide from 1994 to 2005: a cause for concern. *Lancet* **2005**, *366*, 1175-1181.

6. Glycoside Hydrolases: Advances in Research and Application: 2011 Edition.

7. CDC Web Page, https://www.cdc.gov/mmwr/preview/mmwrhtml/rr4814a1.htm.

8. Parkes, K. E. B.; Ermert, P.; Fässler, J.; Ives, J.; Martin, J. A.; Merrett, J. H.; Obrecht, D.; Williams, G.; Klumpp, K. Use of a pharmacophore model to discover a new class of influenza endonuclease inhibitors., *J. Med. Chem.* **2002**, *46,* 1153− 1164.

9. Dias, A.; Bouvier, D.; Crépin, T.; McCarthy, A. A.; Hart, D. J.; Baudin, F.; Cusack, S.; Ruigrok, R. W. H. The cap-snatching endonuclease of influenza virus polymerase resides in the PA subunit. *Nature*, **2009**, *458*, 914-918.

10. Bauman, J. D.; Patel, D.; Baker, S.; Vijayan, R. S. K.; Xiang, A.; Parhi, A.; Martinez-Sobrido, L.; LaVoie, E. J.; Das, K.; Arnold, E. Crystallographic fragment screening and structure-based optimization yields a new class of influenza endonuclease inhibitors. *ACS Chem. Biol.*, **2013**, *8,* 2501− 2508.

11. te Velthuis, A. J. K; Fodor, E. Influenza virus RNA polymerase: insights into the mechanisms of viral RNA synthesis. *Nature Rev. Microbiol.*, **2016**, *14*, 479-493.

12. Fodor, E. The RNA polymerase of influenza A virus: mechanisms of viral transcription and replication. *Acta virologica*, **2013**, *57*, 113-122.

13. ViralZone, https://viralzone.expasy.org/839.

14. Parhi, A.; Xiang, A.; Bauman, J. D.; Patel, D.; Das, K.; Vijayan, R. S. K.; Arnold, E.; LaVoie, E. J. Phenyl substituted 3-hydroxypyridin-2(1*H*)-ones: potential inhibitors of influenza A endonuclease. *Bioorg. Med. Chem.*, **2013**, *21*, 6435− 6446.

15. Sagong, H. Y.; Bauman, J. D.; Patel, D.; Das, K.; Arnold, E.; LaVoie, E. J. Phenyl Substituted 4-Hydroxypyridazin-3(2*H*)-ones and 5-Hydroxypyrimidin-4(3*H*)-ones: Inhibitors of Influenza A Endonuclease. *J. Med. Chem.*, **2014**, *57*, 8086− 8098.

16. Sagong, H. Y.; Parhi, A.; Bauman, J. D.; Patel, D.; Das, K.; Vijayan, R. S. K.; Arnold, E.; LaVoie, E. J. 3-Hydroxyquinolin(1*H*)-2-ones: potential inhibitors of influenza A endonuclease. *ACS Med. Chem. Lett.*, **2013**, *4*, 547− 550.

17. Takahashi C.; Mikumiyama H.; Tomita K.; Taoda Y.; Kawai M.; Anan K.; Miyagawa M.; Suzuki N. Substituted polycyclic carbamoyl pyridone derivative prodrug. US Patent US2013/0197219A1, Aug 1, 2013.

18. Credille, C. V.; Chen, Y.; Cohen, S. M. Fragment-based identification of influenza endonuclease inhibitors. *J. Med. Chem.*, **2016**, *59*, 6444-6454.

19. Baughman, B. M.; Jake Slavish, P.; DuBois, R. M.; Boyd, V. A.; White, S. W.; Webb, T. R. Identification of influenza endonuclease inhibitors using a novel fluorescence polarization assay. *ACS Chem. Biol.*, **2012**, *7*, 526− 534.

20. Wuts, P. G. M.; Greene, T. W. Greene, T. W., & John Wiley & Sons. (2006). Greene's protective groups in organic synthesis. Hoboken, N.J: Wiley-Interscience.

21. N. K. Jana, J. G. Verkade, *Org. Lett.*, **2003**, *5*, 3787-3790.

22. Organic Syntheses, http://orgsyn.org/demo.aspx?prep=CV4P0828.

23. Eugene L. Piatnitski Chekler, Reeti Katoch-Rouse, Alexander S. Kiselyov, Dan Sherman, Xiaohu Ouyang, Ki Kim, Ying Wang, Yaron R. Hadari, Jacqueline F. Doody, Synthesis and evaluation of heteroaryl-ketone derivatives as a novel class of VEGFR-2 inhibitors, *Bioorganic & Medicinal Chemistry Letters*, **2008**, 18(15), 4344-4347.

24. RCSB PDB, https://www.rcsb.org/structure/4AVQ

25. Stevaert, A.; Nurra, S.; Pala, N.; Carcelli, M.; Rogolino, D.; Shepard, C.; Domaoal, R. A.; Kim, B.; Alfonso-Prieto, M.; Marras, S. A. E.; Sechi, M.; Naesens, L. An

integrated biological approach to guide the development of metal-chelating inhibitors of influenza virus PA endonuclease. *Mol. Pharmacol.*, **2015**, *87*, 323-337.

26. 26. Boivin, S.; Cusack, S.; Ruigrok, R. W. H.; & Hart, D. J., Influenza A Virus Polymerase: Structural Insights into Replication and Host Adaptation Mechanisms. *The Journal of Biological Chemistry*, **2010**, *285*(37), 28411–28417.

27. 27. Vedula M. Sharma, P. Prasanna, K.V. Adi Seshu, B. Renuka, C.V. Laxman Rao, G. Sunil Kumar, C.Prasad Narasimhulu, P. Aravind Babu, R.C. Puranik, D. Subramanyam, A. Venkateswarlu, Sriram Rajagopal, K.B.Sunil Kumar, C.Seshagiri Rao, N.V.S.Rao Mamidi, Dhanvanthri S. Deevi, R. Ajaykumar, R. Rajagopalan, Novel indolo[2,1-b]quinazoline analogues as cytostatic agents: synthesis, biological evaluation and structure–activity relationship, *Bioorganic & Medicinal Chemistry Letters*, **2002**, 12(17), 2303-2307.

28. Erick Cuevas-Yañez, Mario A. García, Marco A. de la Mora, Joseph M. Muchowski, Raymundo Cruz-Almanza, Novel synthesis of α-diazoketones from acyloxyphosphonium salts and diazomethane, *Tetrahedron Letters*, **2003**, 44(26), Pages 4815-4817.

29. Wen-Ming Shu, Jun-Rui Ma, Kai-Lu Zheng, Hui-Ying Sun, Mei Wang, Yan Yang, An-Xin Wu, One-pot synthesis of polyfunctional pyrazoles: an easy access to α-diazoketones from arylglyoxal monohydrates and tosylhydrazine, *Tetrahedron*, **2014**, 70(49), 9321-9329.

30. Tatsuya Toma,Jun Shimokawa, and, and Tohru Fukuyama, N,N‘-Ditosylhydrazine: A Convenient Reagent for Facile Synthesis of Diazoacetates, *Organic Letters*, **2007**, *9* (16), 3195-3197.

31. Audrey Wong, Jeffrey T. Kuethe, and, and Ian W. Davies, A General Synthesis of N-Hydroxyindoles**,** *The Journal of Organic Chemistry,* **2003,** *6* (25), 9865-9866

32. Silva, Joaquim F. M. da, Garden, Simon J., & Pinto, Angelo C; The chemistry of isatins: a review from 1975 to 1999; *Journal of the Brazilian Chemical Society*, **2001**;*12*(3), 273-324.

33. Michel Belley*, Daniel Beaudoin, Petar Duspara, Effiette Sauer, Gabriel St-Pierre, Laird A.; Synthesis and Reactivity of *N*-Hydroxy-2-Amino-3-Arylindoles, **2007,** *Synlett*, (19), 2991-2994.

34. J. Cesar, M. Sollner Dolenc; Trimethylsilyldiazomethane in the preparation of diazoketones via mixed anhydride and coupling reagent methods: a new approach to the Arndt-Eistert synthesis; *Tetrahedron Lett.*, **2001**, 42, 7099-7102.

35. Nicolino Pala, Annelies Stevaert, Roberto Dallocchio, Alessandro Dessì, Dominga Rogolino, Mauro Carcelli, Vanna Sanna, Mario Sechi, and Lieve Naesens; Virtual Screening and Biological Validation of Novel Influenza Virus PA Endonuclease Inhibitors; *ACS Medicinal Chemistry Letters*, **2015**, *6*, (8), 866-871.

36. Jaime Martín-Benito, Juan Ortín, Chapter Four - Influenza Virus Transcription and Replication, Advances in Virus Research, Academic Press, Volume 87, **2013**, 113-137.

APPENDIX I: LIST OF EVALUATED COMPOUNDS WITH RS COMPOUND CODES

Compound Number	Compound Code
4	**RS-1-166**
5	**RS-1-115**
6	**RS-1-136**
7	**RS-1-116**
8	**RS-1-117**
9	**RS-1-118**
10	**RS-1-124**
11	**RS-1-125**
12	**RS-1-128**
13	**RS-1-129**
14	**RS-2-36**
15	**RS-2-6**
16	**RS-2-37**
17	**RS-2-34**
18	**RS-2-52**
19	**RS-2-55**
20	**RS-2-44**
21	**RS-2-48**
22	**RS-2-38**
23	**RS-2-59**
24	**RS-2-82**
25	**RS-2-86**

CHAPTER 2

Targeting MreB protein

Introduction

Bacteria that acquire multidrug-resistance to antibiotics pose a significant emerging worldwide health threat.[1] Infections arising from antibiotic-resistant bacteria are responsible for at least 2 million serious morbidities in the USA every year.[1] Around 23,000 fatalities have been reported as a result of antibiotic resistant infections.[1]

Antibiotics play a vital role in treating serious life-threatening infections. The age of antibiotics began with the discovery of penicillin in 1928. However, emerging resistance to penicillin in 1950s led to discovery of newer beta-lactams. Following the emergence of methicillin-resistant *Staphylococcus aureus* (MRSA), resistance to almost all antibiotics has been observed including robust antibiotics like vancomycin.[2] The cause of this global health crisis is majorly attributed to overuse of antibiotics leading to horizontal gene transfer and mutations. Antibiotics can effectively destroy drug-sensitive bacteria, leaving behind those strains which adapt and survive, ultimately causing resistance. Further, inappropriate prescription in the form of suboptimal dosage or questionable therapeutic benefit can also advance antibiotic resistance by mutagenesis and gene alterations that nullify the impact on the antibiotic's biological target.

One approach is to developing a new class of antibiotic agents that affects a novel biological target in bacteria. Recent research has been focused on agents that interfere with the function of MreB protein in bacteria. MreB is a cytoskeletal protein. It is pivotal to the maintenance of the rod shape of certain bacteria and plays a critical role in cell division

and chromosome segregation.[3] It is believed that MreB is highly conserved in rod shaped bacteria and is absent in eukaryotes, making it a sensible target associated with the development of novel antibiotics.[3]

Structure and function of MreB

MreB is a prokaryotic homolog of the protein actin.[4] The structure and function of MreB is not completely elucidated yet. In gram-negative bacteria, like *Escherichia coli*, only a single form of this protein has been observed.[4] In gram-positive bacteria, like *Bacillus subtilis*, numerous MreB forms exist.[4] As a member of the same superfamily of proteins as actin, it has similarity to the structural core of actin. The structure of MreB, as shown in Figure 8 in ribbon form, comprises of domain I and II, with each domain further dividing into subdomains A and B. IA and IIA are the larger subdomains comprising of 3 α-helical structures, which surround a five strand β-sheet.[5] The smaller subdomains IB and IIB are structurally diverse throughout the superfamily with MreB having a similar topology as actin. The cleft between domains I and II holds a nucleotide-binding site and a divalent cation binding site.[5]

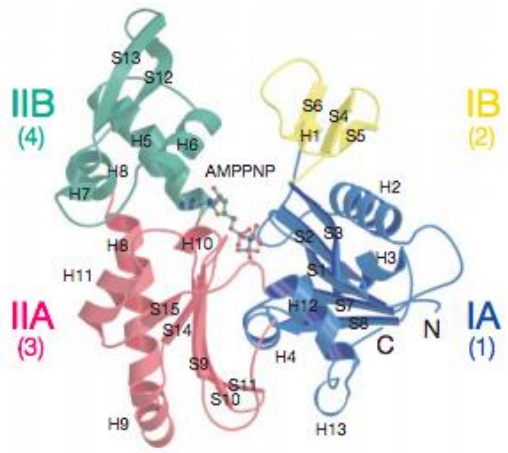

Figure 8. Ribbon form of MreB crystal structure[5]

Similarities between the characteristic structural properties of actin and MreB explain the function of MreB in cell-shape determination. Since MreB is an ATPase protein, it requires ATP to cause polymerization which in turn forms filaments. These filaments are essential in cell-wall synthesis and establishment/maintenance of cell shape. In a normal functioning bacterial cell, polymerization of MreB leads ATP to hydrolyze, which in turn acts as a regulatory timing mechanism to induce depolymerization.[4,5] MreB is also known to contribute to chromosome segregation and cell polarity in a variety of bacteria.[4,5] The importance of MreB in bacterial cell cycle growth suggests that MreB can be used as a potential target for the development of antibacterial agents.[4,5]

MreB Inhibitors

S-(3,4-Dichlorobenzyl) isothiourea (**A22**) (structure illustrated in Figure 9) was discovered from randomized screening for agents that inhibited bacterial chromosome partitioning.[6] It was observed that **A22** modified the shape of rod-shaped bacteria and produced spherical and anucleate cells by asserting an effect on the formation of filaments

by MreB polymerization.[6] It was thought that **A22** inhibits ATP binding by competing at the nucleotide-binding site of MreB.[3,6]

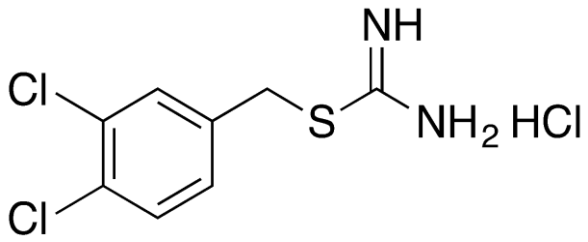

Figure 9. Structure of Compound **A22**[3]

However, studies on the crystal structure of MreB complexed with **A22** and a nonhydrolyzable ATP analog phosphoaminophosphonic acid-adenylate ester (AMPPNP) revealed that **A22** binds to a pocket adjacent to the nucleotide-binding site of MreB.[3]

There remain questions concerning mechanism of MreB inhibition by **A22**. Several hypotheses were put forward.[3] Simulations using molecular dynamics (MD) were used to study interactions at the MreB active site in free and **A22**-ATP bound states.[3] Upon detailed analysis of these simulations, observations were made about the binding of **A22** in the protein pockets that resulted in the elucidation of the mechanism of inhibition of MreB by **A22**.[3]

Observations

1. The phenyl ring of **A22** having two chlorine substituents *meta* and *para* to the thiourea moiety was found to fit into the hydrophobic pocket of MreB. It further interacted with Leu17, Gly18, Met74, Ile79, Phe82, Val109, Pro112, Ala115 and

Ile123. Further, the conformation of this dichlorobenzyl moiety when bound to the protein was found to be similar to the crystal structure of **A22**.

2. The isothiourea functional group was found to engage in hydrogen bond interactions with the γ-phosphate group of ATP by undergoing conformational changes. Also, the isothiourea can flip around the sulfur atom which imparts flexibility in its binding configurations in the protein binding site.

Rationale

Upon carrying out extensive literature survey, we wanted to validate **A22**'s biological activity **A22** was synthesized in our lab. Minimal inhibitory concentrations (MIC) of **A22** and all other following analogs were determined by broth microdilution methods in accordance with Clinical and Laboratory Standards Institute (CLSI) guidelines in the absence or presence of efflux pump inhibitor (EPI) **YZZ-9-155** (structure shown in Figure 10). The tested bacterial strains were *P. aeruginosa PAO1*. Log-phased bacteria were added 96-well microtiter plates (approximately 1 x 10^6 colony forming units per mL) containing two-fold serial dilutions of compounds in cation-adjusted Mueller-Hinton (CAMH) broth (Becton, Dickinson and Co., Franklin Lakes, NJ) in the absence or presence of **YZZ-9-155** at a concentration of 12.5 µg/mL. The final volume in each well was 0.1 mL, and the microtiter plates were incubated aerobically for 24 hours at 37 °C. Bacterial growth was then monitored by measuring the optical density (OD) at 600 nm using a VersaMax® plate reader (Molecular Devices, Inc.), with the MIC being defined as the lowest compound concentration at which growth was ≥ 90% inhibited. Each compound was tested in duplicate. Levofloxacin was included as a positive control for *P. aeruginosa*.

When the assay was carried out in the presence of EPI, if the intrinsic MIC of the EPI is greater than 100 µg/mL, the EPI assay was tested with 50 µg/mL. Using serial dilutions of the EPI, its enhancement of antibiotic activity was then evaluated. The relative EPI activity was decided by comparing the MIC of the antibiotic in the presence of the EPI compound with the intrinsic MIC of the antibiotic alone.

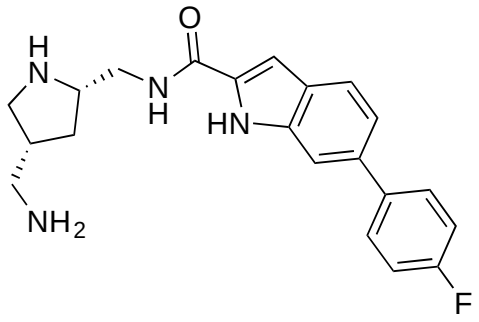

Figure 10. Structure of EPI **YZZ-9-155**

After confirming the inhibitory activity of **A22**, we decided to experiment with a series of side chains with the aromatic core same as **A22**. Activities of several **A22** analogs synthesized in initial phase of this project are tabulated in Table 8.

		P. aeruginosa PAO1	
Compound Number	Structure	Intrinsic MIC (μg/mL)	MIC with 12.5 μg/mL of EPI
A22 (YS-2-148)	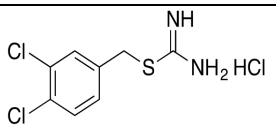	>256	0.5
HY-10-116	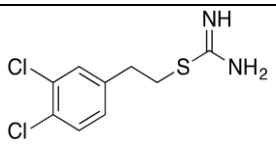	>256	>256
YS-2-156	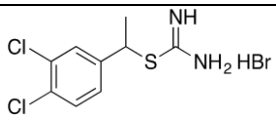	>256	4.0
YS-2-150	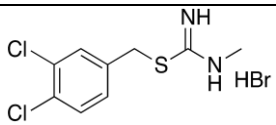	>256	4.0

Table 8. Biological activities of **A22** side chain analogs

Elongation of the methylene side chain by one carbon in **HY-10-116** led to complete loss of activity. Replacement of a methylene hydrogen with a methyl substituent in **YS-2-156** resulted in a higher MIC of 4.0 μg/mL in *P. aeruginosa* when tested in combination with EPI **YZZ-9-155** which suggested eight-fold loss in activity compared to **A22**. Conversion of the primary amine of isothiourea in **YS-2-150** to a secondary amine also resulted in an eight-fold decrease in activity. As a result of these studies, we decided not to modify the isothiourea side chain.

We decided, upon realizing the importance of the presence of a hydrophobic group on the X and Y position of the phenyl ring, to explore additional aryl and heteroaryl groups. We synthesized a series of fused heterocyclic compounds with the isothiourea moiety on

the benzo-ring and the heterocyclic ring fused *meta* and *para* to the isothiourea, resembling X and Y points of attachment of **A22**. These **A22** analogs are outlined in Figure 11.

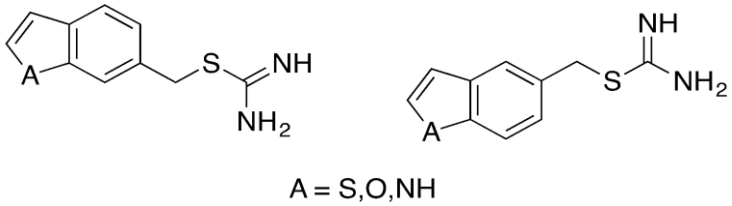

Figure 11. Alternative hydrophobic scaffolds based on **A22**

The relative MICs of these derivatives in the presence and absence of a bacterial efflux pump inhibitor (EPI) are tabulated in Table 9. Based on data shown in Table 9, it was found that benzothiophenes and benzofurans were among the more potent heterocyclic isothiourea derivatives that were assayed. To further advance these structure activity

		P. aeruginosa PAO1	
Compound Number	Structure	Intrinsic MIC (μg/mL)	MIC with 12.5 μg/mL of EPI
A22 (YS-2-148)	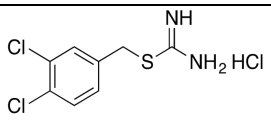	>256	0.5
HY-10-125	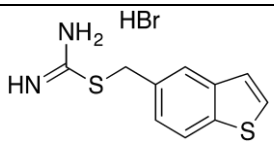	>256	4
HY-10-132	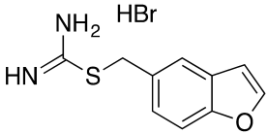	16	4
HY-10-135	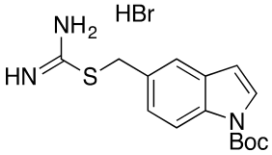	>256	>256

Table 9. Biological activities of A22 heterocyclic analogs in *P. aeruginosa PAO1*

relationships, we also wanted to compare the effect of having the isothiourea substitution on the heterocyclic ring as compared to having the isothiourea on the benzo-ring. Efforts were specifically focused on investigation of the effect of substitution on both the 2 and 3 positions of these three benzo-fused five membered heterocycles. The compounds of interest are summarized in Figure 12. We decided to explore these position isomers along with synthesis of structurally-related indole derivatives as well. The initial synthetic approach that we investigated involved the use of a good leaving group on the methyl substituent, like a halide and displacing it by nucleophilic substitution using thiourea.

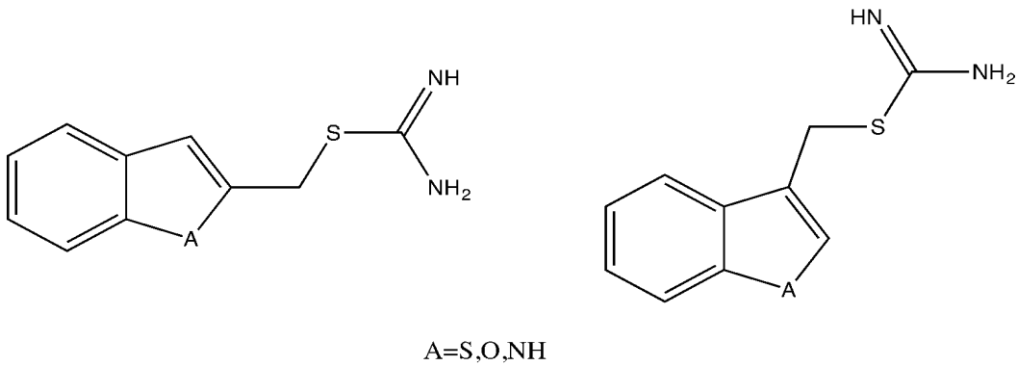

Figure 12. Hydrophobic scaffolds with pharmacophore on heteroatomic ring system

Results and Discussion

a) Benzothiophenes

We started with the synthesis of **28a** from commercially-available 2-methylbenzo[*b*]thiophene using free-radical bromination with N-bromosuccinimide (NBS) and azobisisobutyronitrile (AIBN) as the initiator. Further substitution with thiourea resulted in compound **28** (Scheme 22). The same scheme was successfully used for synthesis for compound **29** (Scheme 22).

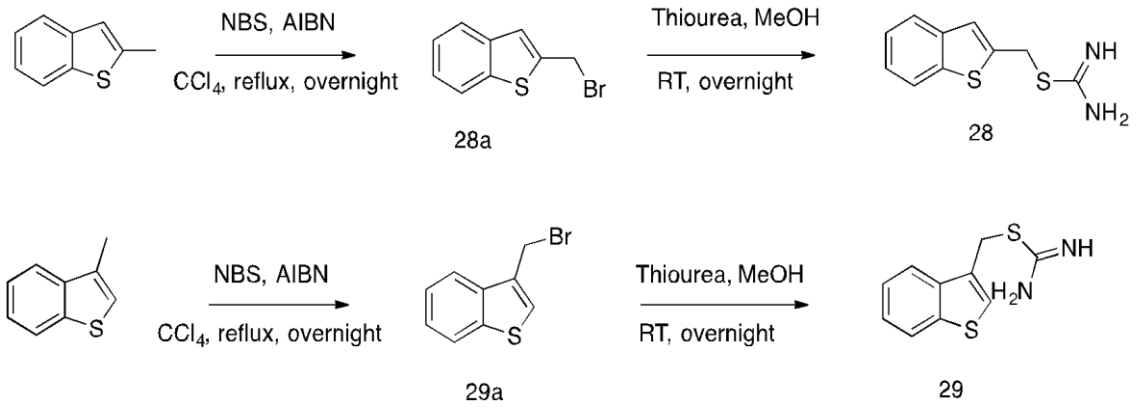

Scheme 22. Synthesis of **28** and **29**

The *in vitro* test data on the antimicrobial activity of **28** and **29** relative to A22 are provided in Table 8. The gram-negative bacteria used in these assays were *P. aeruginosa* PAO1 and *E. coli* ATCC 25922.

	P. aeruginosa PAO1	
Compound	Intrinsic MIC (μg /mL)	MIC (μg/mL) with 12.5 μg/mL EPI
A22	>256	0.5
28	>64	>64
29	>256	16

Table 10. Biological activity of **28** and **29**

Compound **29** showed appreciable inhibitory activity when used in combination with the efflux pump inhibitor (EPI), **YZZ-9-155** in *P. aeruginosa*. This indicated that placement of isothiourea at the 3-position was associated with MreB inhibition and antibacterial activity.

b) Benzofurans

Initially, the same procedure as used to prepare the benzothiophenes **28** and **29** was explored for the synthesis for preparing the structurally-related benzofuran derivatives.

Synthesis of 2-(bromomethyl)benzofuran from 2-methylbenzofuran using NBS bromination, however, was unsuccessful. It was then decided to start with a commercially-available benzofuran-2-ylmethanol and carry out bromination using either hydrobromic acid (33% in acetic acid) or phosphorous tribromide.[7,8] These methods as outlined in Scheme 23 were unsuccessful and in the latter two attempts resulted in destruction of the starting material.

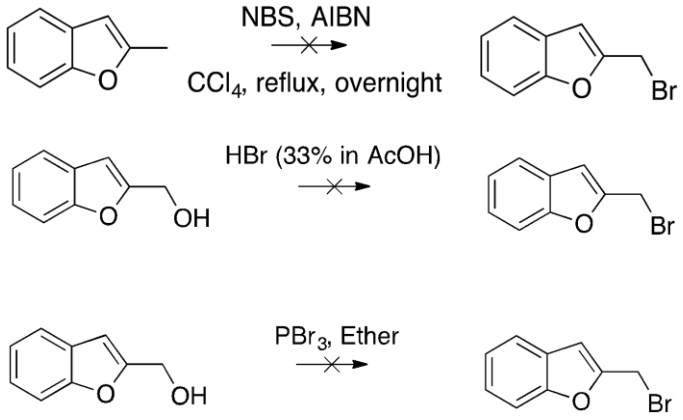

Scheme 23. Attempted synthesis of **30a**

We were ultimately successful in synthesizing 2-(bromomethyl)benzofuran (**30a**) from benzofuran-2-ylmethanol using tetrabromomethane and triphenylphosphine (Scheme 24).[9] Substitution of the bromide with thiourea provided compound **30**.

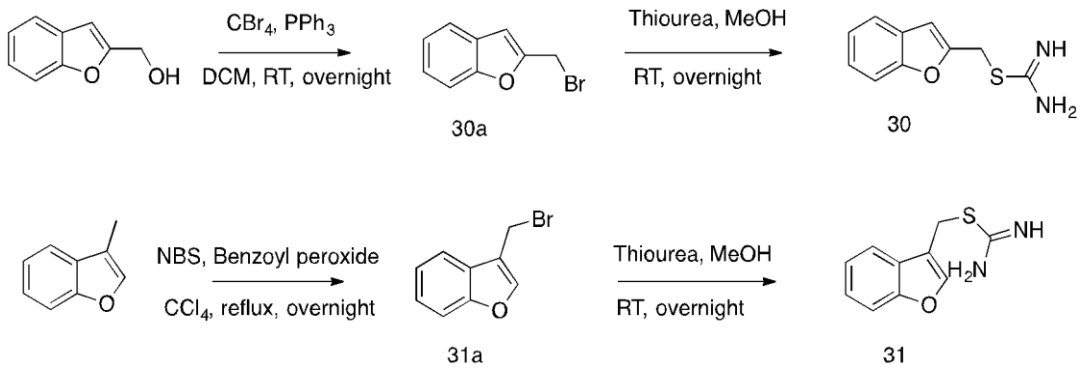

Scheme 24. Synthesis of **30** and **31**

Intermediate **31a** was synthesized using NBS bromination and benzoyl peroxide as the radical chain reaction initiator. This bromomethyl derivative was then used to prepare compound **31** (Scheme 24**)**.

The assay provided in Table 11 revealed **30** to be active against *P. aeruginosa.* These results were not consistent with the results obtained for the benzothiophene **29**. There was a direct opposite effect between the positional isomers in the benzothiophene series with the 3-isothiourea having greater activity than the 2-isothiourea derivative against *P. aeruginosa* PAO1.

	P. aeruginosa PAO1	
Compound	Intrinsic MIC (μg /mL)	MIC (μg/mL) with 12.5 μg/mL EPI
A22	>256	0.5
30	>256	16
31	>64	>64

Table 11. Biological activity of **30** and **31**

c) Indoles

NBS bromination of 2-methylindole and 3-methylindole failed and starting material was recovered unless the –NH hydrogen was protected. The most stable and feasible choice of protecting agent was to form the N-Boc derivatives through the use of di-*tert*-butyl dicarbonate.[10] Ethyl indole-2-carboxylate was reacted with di-*tert*-butyl dicarbonate using 4-dimethylaminopyridine as a nucleophilic catalyst to yield **32a** in quantitative yield as shown in Scheme 25. Reduction of **32a** using DIBAL-H at -40 °C provided the alcohol **32b**. Bromination of **32b** using a mild Lewis acid agent such as lithium bromide via formation of sulfonate using mesyl chloride yielded an unstable bromo intermediate was subjected to nucleophilic substitution using thiourea to give boc-protected isothiourea **32c** which on acidic deprotection using TFA: CH_2Cl_2 gave product **32**.

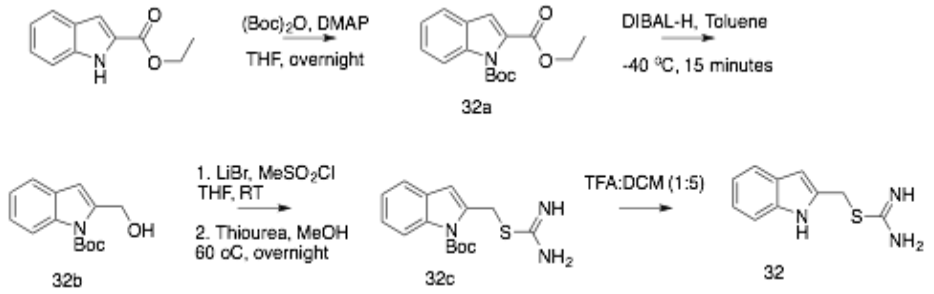

Scheme 25. Synthesis of **32**

Compound **33** was synthesized in a straightforward manner by starting with the commercially-available boc-protected halide as illustrated in Scheme 26. Nucleophilic substitution with thiourea gave **33a** in 35% yield and further deprotection by treating with TFA: CH_2Cl_2 for 15 minutes provided **33**.

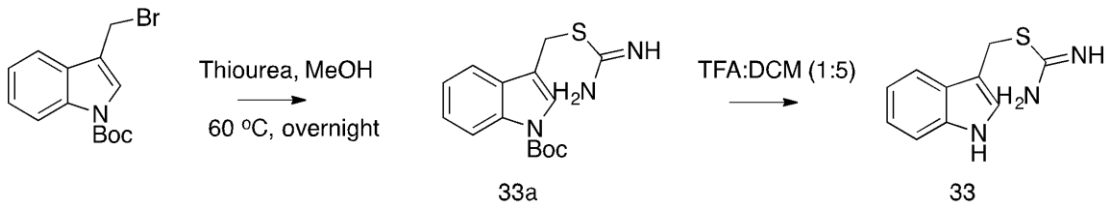

Scheme 26. Synthesis of **33**

Synthesis of N-methyl derivatives of indole isothioureas was viewed essential for completion of the structure-activity-relationships within this series. Efforts began with protection of the hydroxyl group of ethylindole-2-methanol by forming the *tert*-butyldimethyl silyl protecting group as shown in Scheme 27. Upon NMR analysis, it was surprisingly discovered that the free hydrogen on -NH got protected instead of the –OH.

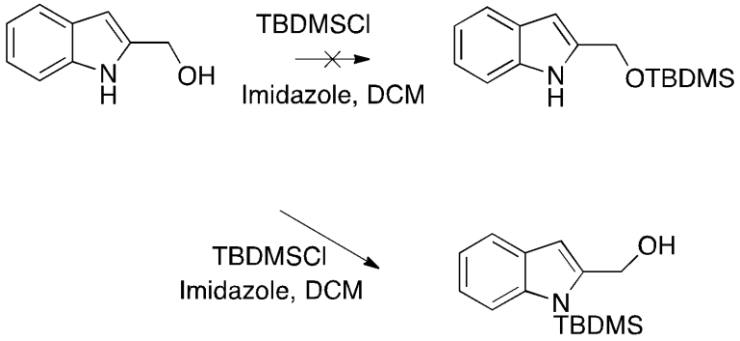

Scheme 27. Attempted synthesis I of intermediate for **34**

Hence, it was thought best to start with an alternative substrate like ethylindole-2-carboxylate. N-methylation of the carboxylate and subsequent reduction using DIBAL-H yielded the N-methylated alcohol **34a** as illustrated in Scheme 28. Bromination of **34a**, however, failed when HBr or PBr_3 was used.

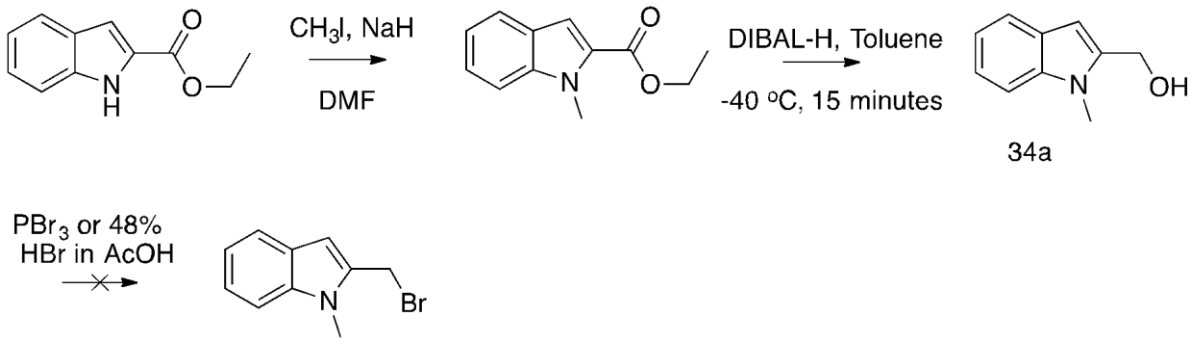

Scheme 28. Attempted synthesis of **34**

Finally, we started with the commercially-available 1-methyl-1*H*-indole-2-carbaldehyde and carried out its reduction using DIBAL-H as illustrated in Scheme 29. Bromination of the resulting alcohol using tetrabromomethane and triphenylphosphine gave the bromide **34a**. Reaction of crude **34a** with thiourea provided compound **34**.

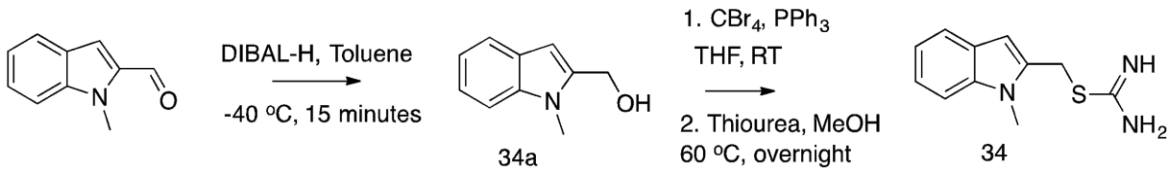

Scheme 29. Synthesis of **34**

Compound **32** and its Boc protected derivative **32c** both exhibited growth inhibitory activity *in vitro* against *P. aeruginosa* as shown in Table 12 when assayed in combination with the bacterial efflux pump inhibitor YZZ-9-155. Formation of its N-methyl derivative, **34**, resulted in a loss of activity.

	P. aeruginosa PAO1	
Compound	Intrinsic MIC (μg /mL)	MIC (μg/mL) with 12.5 μg/mL EPI
A22	>256	0.5
32c	64	16
32	128	16
33a	>256	>256
33	>256	>256
34	>256	>256

Table 12. Biological activity of **32c-34**

Using data derived from assay studies on all three series, it was deduced that the 2nd position on the heterocycle was more effective than the 3rd position.

SUMMARY

The emergence of antibiotic-resistance crisis on a global scale calls for the development of a new drugs that are fundamentally unique in their mode of action from the current antibiotics. MreB, a cytoskeletal actin-like protein is crucial in the bacterial cell life cycle and in maintaining cell shape of bacteria, making it a potential target for design of novel antibiotics.

The isothiourea based bacteriostatic inhibitor, A22, acts by disrupting the function of MreB, leading to a loss of cell shape in bacteria. The structure and mechanism of action of A22 inspired the development of series of heterocyclic isothioureas. The heterocycles evaluated included benzothiophenes, benzofurans and indoles. The effect of substitution of isothiourea at various positions on the heterocyclic portion of these molecules and its effect on the inhibitory activity was studied. Compounds **29**, **30**, **32c** and **32** were found to inhibit *P. aeruginosa* PAO1 strain with an MIC of 16 μg /mL when used in conjunction with the bacterial efflux pump inhibitor **YZZ-9-155**.

In conclusion, this chapter of dissertation describes the synthesis, SAR and biological evaluation of potential MreB inhibitors as antibiotics in specific bacterial strains. Current efforts of the laboratory are focused on developing a highly optimized lead compound based on present SAR data, that can potentially be developed into the clinic.

EXPERIMENTAL

General

Reactions were monitored using aluminum baked silica G TLC plates (Sorbent Technologies) with UV254 and visualized under ultraviolet light. Purification was done using Combi Flash Rf Teledyne ISCO flash chromatography system with 230-400 mesh silica gel columns (Teledyne ISCO). Solvents ethyl acetate (EtOAc), hexane, methanol (MeOH) or dichloromethane (CH_2Cl_2) were purchased from Sigma-Aldrich, Inc., USA and used as indicated in each procedure. NMR spectra, both proton ^1H (400 MHz) and carbon ^{13}C (100 MHz), were recorded using Bruker Avance III (400 MHz) Multinuclear NMR Spectrometer. Deuterated solvents ($CDCl_3$, DMSO-d_6) were purchased from Cambridge Isotopes Laboratory (Cambridge, MA). Chemical shift data was expressed in parts per million (δ) relative to residual nondeuterated solvent signal. Spin multiplicities were abbreviated as s (singlet), d (doublet), dd (doublet of doublets), t (triplet), dt (doublet of triplets), td (triplet of doublets), q (quartet), sep (septet), m (multiplet), brs (broad singlet). Coupling constants were reported in Hertz (Hz). Melting points (uncorrected) were calculated using Mel-temp II apparatus.

2-(Bromomethyl)benzo[*b*]thiophene (**28a**)

2-Methylthianaphthene (200 mg, 1.35 mmol) was dissolved in carbon tetrachloride and N-bromosuccinimide (240 mg, 1.35 mmol) and azobisisobutyronitrile (22 mg, 0.135 mmol) was added. The mixture was refluxed overnight. Solvent was evaporated under reduced pressure once the reaction completed and product was purified using an ISCO (10% ethyl acetate in hexanes) to yield 45 mg (15%) of **28a**. ^1H NMR (400 MHz) ($CDCl_3$) δ 7.70 (t, *J*

= 4 Hz, 1H), 7.64 (t, *J* = 8 Hz, 1H), 7.24-7.27 (m, 3H), 4.70 (s, 2H); ^{13}C NMR (100 MHz) ($CDCl_3$) δ 141.1, 139.4, 139.2, 124.4, 124.2, 123.3, 122.8, 122.3, 27.5

Benzo[*b*]thiophen-2-ylmethyl carbamimidothioate (**28**)

2-(Bromomethyl)benzo[*b*]thiophene (**28a**) (45 mg, 0.19 mmol) was dissolved in methanol and thiourea (14 mg, 0.19 mmol) was added. The mixture was stirred at room temperature overnight. Mixture was diluted with ethyl acetate and washed with water, followed by brine. Organic layer was dried over sodium sulfate, solvent evaporated under reduced pressure and crude product was purified using an ISCO (10% methanol in CH_2Cl_2) to obtain 32 mg (76%) of 28 as a white powder. ^{1}H NMR (400 MHz) (DMSO) δ 7.88 (d, *J* = 8 Hz, 1H), 7.75 (d, *J* = 8 Hz, 1H), 7.28-7.36 (m, 3H), 4.48 (s, 2H); ^{13}C NMR (100 MHz) (DMSO) δ 139.4, 139.1, 124.4, 124.3, 124.1, 124.0, 123.3, 122.4, 122.2, 36.8

Benzo[*b*]thiophen-3-ylmethyl carbamimidothioate (**29**)

3-Methylthianaphthene (200 mg, 1.35 mmol) was dissolved in carbon tetrachloride. N-bromosuccinimide (240 mg, 1.35 mmol) and azobisisobutyronitrile (22 mg, 0.135 mmol) was added to the solution. The mixture was refluxed overnight. Upon completion of reaction, the solvent was evaporated under reduced pressure and crude product **29a** was taken ahead to next step. 3-(bromomethyl)benzo[*b*]thiophene (**29a**) (45 mg, 0.56 mmol) was dissolved in methanol and thiourea (43 mg, 0.56 mmol) was added. The mixture stirred at room temperature overnight. Mixture was diluted with ethyl acetate and washed with water, followed by brine. Organic layer was dried over sodium sulfate, solvent evaporated under reduced pressure and crude product was purified on an ISCO (10% methanol in

CH_2Cl_2) to obtain 32 mg (76%) of 29 as a white powder. ^{1}H NMR (400 MHz) (DMSO) δ 7.99 (d, *J* = 4 Hz, 1H), 7.92 (d, *J* = 4 Hz, 1H), 7.67 (s, 1H), 7.38-7.45 (m, 2H), 4.42 (s, 2H); ^{13}C NMR (100 MHz) (DMSO) δ 140.4, 140.1, 124.4, 124.3, 124.2, 124.1, 122.8, 122.3, 122.2, 35.8

Benzofuran-2-ylmethyl carbamimidothioate (**30**)

1-Benzofuranyl-2-methanol (200 mg, 1.35 mmol) was dissolved in CH_2Cl_2. Tetrabromomethane (448 mg, 1.35 mmol) and 262 mg of triphenylphosphine (1.35 mmol) was added at 0 °C. The reaction mixture was stirred for two hours at room temperature, solvent was evaporated using reduced pressure and crude **30a** was dissolved in methanol. Thiourea (103 mg, 1.35 mmol) was added and the mixture was stirred overnight at 60 °C. The organic layer was evaporated under reduced pressure and crude product purified on column using an ISCO (10% methanol in CH_2Cl_2) to yield 100 mg (36%) of 30 as a white powder. mp 184-186 °C; ^{1}H NMR (400 MHz) (DMSO) δ 9.30 (brs, 1H), 9.10 (brs, 1H), 7.64 (d, *J* = 8 Hz, 1H), 7.56 (d, *J* = 8 Hz, 1H), 7.33 (t, *J* = 8 Hz, 1H), 7.26 (t, *J* = 8 Hz, 1H), 6.93 (s, 1H), 4.78 (s, 2H); ^{13}C NMR (100 MHz) (DMSO) δ 168.3, 154.4, 151.6, 127.6, 124.7, 123.1, 121.3, 111.0, 105.9, 27.6

Benzofuran-3-ylmethyl carbamimidothioate (**31**)

3-Methylbenzofuran (500 mg, 3.78 mmol) was dissolved in carbon tetrachloride. N-bromosuccinimide (678 mg, 3.78 mmol) and benzoyl peroxide (92 mg, 0.38 mmol). The mixture was refluxed overnight. Upon completion of reaction, the solvent was evaporated under reduced pressure to yield 825 mg of crude 2-(bromomethyl)benzofuran (**31a**). Crude

31a was dissolved in methanol and thiourea (297 mg, 3.9 mmol) was added to the solution. The mixture was stirred overnight at 60 °C. Mixture was diluted with ethyl acetate and washed with water, followed by brine. Organic layer was dried over sodium sulfate, solvent evaporated under reduced pressure and crude product was purified on an ISCO (10% methanol in CH_2Cl_2) to obtain 50 mg (7%) of pure **31** as a white salt. 185-187 °C dec; ^{1}H NMR (400 MHz) (DMSO) δ 7.81 (s, 1H), 7.70 (d, *J* = 8 Hz, 1H), 7.59 (d, *J* = 8 Hz, 1H), 7.35 (t, *J* = 8 Hz, 1H), 7.30 (t, *J* = 8 Hz, 1H), 6.63 (brs, 3H), 3.96 (s, 2H); ^{13}C NMR (100 MHz) (DMSO) δ 154.7, 143.9, 126.4, 124.6, 122.6, 120.2, 115.9, 111.4, 30.4

tert-Butyl 2-(hydroxymethyl)-1*H*-indole-1-carboxylate (**32b**)

Ethylindole-2-carboxylate (1.0 g, 5.28 mmol) was dissolved in anhydrous THF. Di-*tert*-butyl dicarbonate (1.26 g, 5.8 mmol) and 4-dimethylaminopyridine (71 mg, 0.58 mmol) was added to the solution and the mixture was stirred at room temperature overnight. Reaction mixture was diluted with CH_2Cl_2 upon completion and then washed with water, saturated ammonium chloride solution, followed by brine. The organic layer was dried over sodium sulfate and solvent evaporated under reduced pressure to yield 1.53 g of crude **32a**. Crude **32a** was then dissolved in toluene and DIBAL-H (1.9 g, 13.2 mmol) was added to the solution. The mixture was stirred at -40 °C for 20 minutes, then methanol (3 mL) and water (1.5 mL) was added. The reaction mixture was stirred at room temperature for 15 minutes, filtered and the filtrate was extracted with CH_2Cl_2 and water. The organic layer was dried over sodium sulfate and the solvent evaporated under reduced pressure to obtain 320 mg (25%) of **32b**. ^{1}H NMR (400 MHz) ($CDCl_3$) δ 7.99 (d, *J* = 8 Hz, 1H), 7.51 (d, *J* = 8 Hz, 1H), 7.29 (t, *J* = 8 Hz, 1H), 7.22 (t, *J* = 8 Hz, 1H), 6.58 (s, 1H), 4.81 (d, *J* = 8 Hz,

1H); ^{13}C NMR (100 MHz) ($CDCl_3$) 146.1, 135.0, 131.0, 123.7, 119.1, 117.8, 110.4, 104.4, 53.7

tert-Butyl 2-((carbamimidoylthio)methyl)-1*H*-indole-1-carboxylate (**32c**)

tert-Butyl 2-(hydroxymethyl)-1*H*-indole-1-carboxylate (**32b**) (320 mg, 1.29 mmol) was dissolved in THF. Lithium bromide (1.1 g, 12.9 mmol), triethylamine (0.45 mL, 3.22 mmol) and methanesulfonyl chloride (295 mg, 2.58 mmol) was added and the mixture was stirred overnight at room temperature. Solvent was removed under reduced pressure and the crude product was then dissolved in methanol. Thiourea (98 mg, 1.29 mmol) was added and the reaction was stirred at 60 °C overnight. Reaction mixture was filtered to obtain 136 mg (35%) of precipitated product as a buff colored powder **32c**. 143-145 °C mp; ^{1}H NMR (400 MHz) (DMSO) δ 9.28 (brs, 4H), 8.05 (d, *J* = 8 Hz, 1H), 7.61 (d, *J* = 8 Hz, 1H), 7.34 (t, *J* = 8 Hz, 1H), 7.25 (t, *J* = 8 Hz, 1H), 6.89 (s, 1H), 4.86 (s, 2H), 1.67 (s, 9H); ^{13}C NMR (100 MHz) (DMSO) δ 168.8, 149.4, 136.1, 134.1, 127.9, 124.7, 123.1, 120.8, 115.3, 110.4, 85.0, 29.6, 27.6

(1*H*-indol-2-yl)methyl carbamimidothioate (**32**)

tert-Butyl 2-((carbamimidoylthio)methyl)-1*H*-indole-1-carboxylate (**32c**) (98 mg, 0.35 mmol) was dissolved in CH_2Cl_2 and trifluoroacetic acid in CH_2Cl_2 (1 mL:5 mL) dropwise was added. The solution was stirred at room temperature for 15 minutes. Solvent was removed under reduced pressure and residue washed with CH_2Cl_2. The crude product was purified using an ISCO (10% methanol in CH_2Cl_2) to yield 51 mg (71%) of **32** as a

buff colored solid. mp 131-133 °C; ^{1}H NMR (400 MHz) (DMSO) δ 9.29 (brs, 4H), 7.49 (d, *J* = 8 Hz, 1H), 7.36 (d, *J* = 8 Hz, 1H), 7.09 (t, *J* = 8 Hz, 1H), 6.99 (t, *J* = 8 Hz, 1H), 6.46 (s, 1H), 4.65 (s, 2H); ^{13}C NMR (100 MHz) (DMSO) δ 168.9, 136.5, 131.8, 127.5, 121.6, 119.9, 119.2, 111.2, 101.8, 27.9

tert-Butyl 3-((carbamimidoylthio)methyl)-1*H*-indole-1-carboxylate (**33a**)

tert-butyl 3-(bromomethyl)-1*H*-indole-1-carboxylate (200 mg, 0.65 mmol) was dissolved in methanol and thiourea (50 mg, 0.65 mmol) was added. The mixture was stirred at 60 °C for 3 hours. The solvent was removed under reduced pressure and crude product was purified on an ISCO (5% methanol in CH_2Cl_2) to obtain 70 mg (35%) of **33a** as a brown oil. ^{1}H NMR (400 MHz) (DMSO) δ 9.08 (brs, 4H), 8.06 (d, *J* = 8 Hz, 1H), 7.81 (s, 1H), 7.77 (d, *J* = 8 Hz, 1H), 7.39 (t, *J* = 8 Hz, 1H), 7.32 (t, *J* = 8 Hz, 1H), 4.67 (s, 2H), 1.64 (s, 9H); ^{13}C NMR (100 MHz) (DMSO) δ 168.8, 149.4, 136.1, 134.1, 127.9, 124.7, 123.1, 120.8, 115.3, 110.4, 85.0, 29.6, 25.6

(1*H*-Indol-3-yl)methyl carbamimidothioate (**33**)

tert-Butyl 3-((carbamimidoylthio)methyl)-1*H*-indole-1-carboxylate (**33a**) (30 mg, 0.09 mmol) was dissolved in CH_2Cl_2 and trifluoroacetic acid in CH_2Cl_2 (1:1) was added in a dropwise manner. The solution was stirred at room temperature until a precipitate was observed (about 15 minutes). The precipitate was filtered to obtain 14 mg (77%) of pure product **33**. mp 102-104 °C; ^{1}H NMR (400 MHz) (DMSO) δ 9.06 (brs, 4H), 7.65 (d, J = 8 Hz, 1H), 7.45 (s, 1H), 7.41 (d, J = 8 Hz, 1H), 7.14 (t, J = 8 Hz, 1H), 7.06 (t, J = 8 Hz, 1H),

4.70 (s, 2H); ^{13}C NMR (100 MHz) (DMSO) δ 169.8, 136.2, 126.0, 125.5, 124.1, 119.0, 118.4, 111.8, 106.4, 27.1

(1-Methyl-1*H*-indol-2-yl)methyl carbamimidothioate (**34**)

1-Methyl-1*H*-indole-2-carboxaldehyde (500 mg, 3.14 mmol) was dissolved in methanol and sodium borohydride (130 mg, 3.45 mmol) was added in portions at 0 °C. The mixture was stirred at room temperature and monitored on TLC. Upon completion, the mixture was extracted using ethyl acetate, saturated ammonium chloride solution and brine. The organic layer was dried over sodium sulfate and evaporated under reduced pressure to obtain 480 mg (96%) of crude **34a** as a yellow waxy solid which was taken to the next step. **34a** (200 mg, 1.24 mmol) was dissolved in CH_2Cl_2. Tetrabromomethane (411 mg, 1.24 mmol) and triphenylphosphine (325 mg, 1.24 mmol) was added and the mixture was stirred overnight at room temperature. The solvent was removed under reduced pressure and the crude intermediate dissolved in methanol. To this solution was added thiourea (94 mg, 1.24 mmol) and the mixture stirred at 60 °C overnight until a precipitate was observed. The precipitate was filtered to obtain 42 mg of pure product **34** as a brown powder. 230-232 °C dec; ^{1}H NMR (400 MHz) (DMSO) δ 7.66 (d, *J* = 8 Hz), 7.40 (d, J = 8 Hz), 7.12 (t, J = 8 Hz, 1H), 7.00 (t, J = 8 Hz, 1H), 5.41 (s, 1H), 5.06 (d, J = 4 Hz, 1H), 3.78 (s, 3H); ^{13}C NMR (100 MHz) (DMSO) δ 142.0, 136.6, 128.3, 121.8, 119.5, 119.1, 109.7, 103.3, 52.9, 30.2

REFERENCES

1. Antibacterial agents in clinical development, http://apps.who.int/iris/bitstream/10665/258965/1/WHO-EMP-IAU-2017.11-eng.pdf?ua=1.

2. Ventola CL. The Antibiotic Resistance Crisis: Part 1: Causes and Threats. *Pharmacy and Therapeutics*. **2015**;40(4):277-283.

3. Yaw Awuni, Shimin Jiang, Robert C. Robinson, and Yuguang Mu; Exploring the A22-Bacterial Actin MreB Interaction through Molecular Dynamics Simulations; *The Journal of Physical Chemistry B* **2016** *120* (37), 9867-9874.

4. Gitai, Zemer et al.; MreB Actin-Mediated Segregation of a Specific Region of a Bacterial Chromosome; *Cell*, 2005, 120(3), 329 – 341.

5. Fusinita van den Ent, Linda A. Amos, Jan Löwe, Prokaryotic origin of the actin cytoskeleton; *Nature;* **2001**; 413; 39-44.

6. Noritaka Iwai, Takuya Fujii, Hirokatsu Nagura, Masaaki Wachi & Tomoya Kitazume, Structure-Activity Relationship Study of the Bacterial Actin-Like Protein MreB Inhibitors: Effects of Substitution of Benzyl Group in S-Benzylisothiourea, *Bioscience, Biotechnology, and Biochemistry*, **2007**, 71:1, 246-248.

7. Wing-Yiu Yu, Yuk-Tai Tsoi, Zhongyuan Zhou, and Albert S. C. Chan, Palladium-Catalyzed Cross Coupling Reaction of Benzyl Bromides with Diazoesters for Stereoselective Synthesis of (E)-α,β-Diarylacrylates, *Organic Letters,* **2009,** 11(2), 469-472.

8. Bilger C., Royer R., Demerseman P., A convenient one-pot synthesis of aralkyl bromides and iodides for reductive halogenation of aromatic carbonyl compounds, *Synthesis,* **1988**, 1988(11): 902-904.

9. Aissaoui Hamed, Boss Christoph, Heidmann Bibia, Sifferlen Thierry, Williams Jodi T., Lactam derivatives useful as orexin receptor antagonists and their preparation and use for the treatment of diseases, US Patent US 9,242,970 B2, Jan 26, 2016.

10. Wuts, P. G. M.; Greene, T. W. Greene, T. W., & John Wiley & Sons. (2006). Greene's protective groups in organic synthesis. Hoboken, N.J: Wiley-Interscience.

11. Norihisa Noguchi, Keita Yanagimoto, Hidemasa Nakaminami, Moeru Wakabayashi, Noritaka Iwai, Masaaki Wachi, Masanori Sasatsu, Anti-infectious

Effect of *S*-Benzylisothiourea Compound A22, Which Inhibits the Actin-Like Protein, MreB, in *Shigella flexneri*, *Biological and Pharmaceutical Bulletin;* **2008**, 31(7), 1327-1332.

12. Molshanski-Mor, S., Yosef, I., Kiro, R., Edgar, R., Manor, M., Gershovits, M.; Qimron, U. Revealing bacterial targets of growth inhibitors encoded by bacteriophage T7. *Proceedings of the National Academy of Sciences of the United States of America*, **2014,** *111*(52), 18715–18720.

13. Min Jin, Yanjiang Chen, Chenxi Xu, Xiaobo Zhang; The effect of inhibition of host MreB on the infection of thermophilic phage GVE2 in high temperature environment; *Scientific Reports,* **2014**, 4, 4823.

14. Robertson GT, Doyle TB, Du Q, Duncan L, Mdluli KE, Lynch AS. A Novel Indole Compound That Inhibits *Pseudomonas aeruginosa* Growth by Targeting MreB Is a Substrate for MexAB-OprM. *Journal of Bacteriology*. **2007**; 189(19):6870-6881.

15. G. J. Bean, S. T. Flickinger, W. M. Westler, M. E. McCully, D. Sept, D. B. Weibel, and K. J. Amann, A22 Disrupts the Bacterial Actin Cytoskeleton by Directly Binding and Inducing a Low-Affinity State in MreB, *Biochemistry* **2009** *48* (22), 4852-4857.

16. Gitai Z., Shapiro L., Wachi M., Iwai N., Antibiotics targeting MreB, US Patent US 7,855,228 B2, Dec. 21, 2010.

17. Figge R., Divakarini A., Gober J., MreB, the cell shape determining bacterial actin homologue, co-ordinates cell wall morphogenesis in *Caulobacter crescentus*, *Molecular Microbiology*, **2004,** 51(5), 1321-1332.

APPENDIX II: LIST OF EVALUATED COMPOUNDS WITH THEIR CORRESPONDING RS CODES

Compound Number	Compound Codes
28	**RS-2-100**
29	**RS-2-104**
30	**RS-2-122**
31	**RS-2-115**
32c	**RS-2-159**
32	**RS-2-160**
33c	**RS-2-145**
33	**RS-2-146**
34	**RS-2-170**